# Measurement of prompt open-charm production cross sections in proton-proton collisions at $\sqrt{s} = 13\,\text{TeV}$

## The CMS collaboration

*E-mail:* cms-publication-committee-chair@cern.ch

ABSTRACT: The production cross sections for prompt open-charm mesons in proton-proton collisions at a center-of-mass energy of 13 TeV are reported. The measurement is performed using a data sample collected by the CMS experiment corresponding to an integrated luminosity of $29\,\text{nb}^{-1}$. The differential production cross sections of the $D^{*\pm}$, $D^{\pm}$, and $D^0$ ($\overline{D}^0$) mesons are presented in ranges of transverse momentum and pseudorapidity $4 < p_T < 100\,\text{GeV}$ and $|\eta| < 2.1$, respectively. The results are compared to several theoretical calculations and to previous measurements.

# Contents

# 1   Introduction

Measurements of the production cross sections for open-charm mesons, i.e., mesons containing a single charm quark, in hadronic collisions at LHC center-of-mass energies provide an important test of the theory of strong interactions known as quantum chromodynamics (QCD). Due in part to the presence of several competing scales (charm mass, transverse momentum) that are close to the threshold for the validity of the perturbative expansion, the theoretical uncertainties are rather large. Therefore, experimental constraints on heavy-quark production cross sections are relevant for physics phenomena directly involving heavy quarks or for which they constitute a background. An improved understanding of charm production is furthermore relevant for the exploration of physics processes arising from charm hadron decays, such as neutrinos and other feebly interacting particles [1–3], and as a reference for the study of the properties of QCD extreme media [4]. Several studies have been carried out at the LHC. These include measurements at $\sqrt{s} = 7\,\mathrm{TeV}$ by the ATLAS Collaboration [5], at $\sqrt{s} = 5$ [6, 7], 7 [8, 9], and 13 TeV [10] by the ALICE experiment, and at $\sqrt{s} = 5$ [11], 7 [12], and 13 TeV [13] by the LHCb Collaboration. The CMS experiment has produced results on open-charm production, analyzing heavy-ion and proton-proton (pp) collisions at $\sqrt{s_{\mathrm{NN}}} = 5.02\,\mathrm{TeV}$ [4].

In this paper, a study of charm meson production by CMS in pp collisions at $\sqrt{s} = 13\,\text{TeV}$ is presented. The analysis is focused on the measurement of cross sections for the prompt production of $\text{D}^{*+}$, $\text{D}^0$, and $\text{D}^+$ mesons. The charm mesons are identified via their exclusive decays:

- $\text{pp} \to \text{D}^{*+}X \to \text{D}^0\pi_\text{S}^+X \to \text{K}^-\pi^+\pi_\text{S}^+X$,

- $\text{pp} \to \text{D}^0X \to \text{K}^-\pi^+X$,

- $\text{pp} \to \text{D}^+X \to \text{K}^-\pi^+\pi^+X$,

where $X$ corresponds to any set of possible particles. Charge conjugation is implied throughout the paper, unless specified otherwise. The designation $\pi_\text{S}^+$ indicates that, because of the specific kinematics of the $\text{D}^{*+}$ decay, this "slow" pion has significantly lower momentum than the kaon and pion decay products of the $\text{D}^0$. The $\text{D}^{*+}$, $\text{D}^0$, and $\text{D}^+$ mesons are reconstructed in the range of transverse momentum $4 < p_\text{T} < 100\,\text{GeV}$ and pseudorapidity $|\eta| < 2.1$.

Charm mesons arising from the pp collision point, either directly or as decay products of excited charm resonances (e.g., $\text{D}^0$ coming from $\text{D}^{*+}$ decay), are referred to as promptly produced. Contrarily, charm mesons coming from the decays of b hadrons, e.g., $\text{B} \to \text{D}X$, where $X$ denotes any additional particles, are referred to as nonprompt and are considered as a background process.

Since the kinematic regions covered by the existing measurements differ from the one presented in this paper and are fully complementary in the case of LHCb, the new measurements described in this paper and their comparison to theoretical predictions provide an important contribution to a deeper understanding of the charm production mechanism.

The single-differential cross sections for prompt charm meson production are measured as a function of the transverse momentum $p_\text{T}$ and the absolute value of pseudorapidity $|\eta|$. In principle, rapidity ($y$) is the proper kinematic variable to study cross sections of massive particles. Here, pseudorapidity is used instead of rapidity to facilitate the comparison with the ATLAS measurement [5], which is the closest in kinematic range to the results presented in this paper. In the kinematic phase space of this measurement, the maximum difference between $\eta$ and $y$ is less than 5%. Tabulated results are provided in HEPData [14]. The measured cross sections are compared to the predictions from the Monte Carlo (MC) event generators PYTHIA 6.4 [15] and 8.1 [16], to the theoretical calculations from FONLL [17, 18], and to the previous LHC results [4–6, 8, 9, 11–13].

## 2 The CMS detector

The central feature of the CMS apparatus is a superconducting solenoid of 6 m internal diameter, providing a magnetic field of 3.8 T. Within the solenoid volume are a silicon pixel and strip tracker, a lead tungstate crystal electromagnetic calorimeter, and a brass and scintillator hadron calorimeter, each composed of a barrel and two endcap sections. Forward calorimeters extend the pseudorapidity coverage provided by the barrel and endcap detectors. Muons are detected in gas-ionization chambers embedded in the steel flux-return

yoke outside the solenoid. The most relevant subdetector for this analysis is the silicon tracker. The silicon tracker measures charged particles within the pseudorapidity range $|\eta| < 2.5$. It consists of 1440 silicon pixel and 15 148 silicon strip detector modules. For nonisolated particles of $1 < p_T < 10\,\text{GeV}$ and $|\eta| < 1.4$, the track resolutions are typically 1.5% in $p_T$ and 25–90 (45–150) $\mu$m in the transverse (longitudinal) impact parameters [19].

Events of interest are selected using a two-tiered trigger system [20]. The first level, composed of custom hardware processors, uses information from the calorimeters and muon detectors to select events at a rate of around 100 kHz within a time interval of less than 4 $\mu$s. The second level, known as the high-level trigger, consists of a farm of processors running a version of the full event reconstruction software optimized for fast processing, and reduces the event rate to around 1 kHz before data storage. A more detailed description of the CMS detector, together with a definition of the coordinate system used and the relevant kinematic variables, can be found in ref. [21].

## 3    Data samples, simulation, and event selection

The data sample was acquired in 2016 and corresponds to an integrated luminosity of $29\,\text{nb}^{-1}$, out of the $36.8\,\text{fb}^{-1}$ collected in that year [22]. The average number of simultaneous pp collisions in the same or nearby bunch crossings, referred to as pileup (PU), for the subset of data used for this analysis is 14. To avoid any bias from a trigger requirement that would aim to select events and require an efficiency correction, the data used in this analysis were collected with an unbiased trigger that only required the presence of crossing beams. This trigger was heavily prescaled, which explains the low effective integrated luminosity for this analysis with respect to the total one collected in 2016.

The candidate vertex with the largest value of summed physics object $p_T^2$ is taken to be the primary pp interaction vertex (PV). The physics objects are the jets, clustered using the jet-finding algorithm [23, 24] with the tracks assigned to candidate vertices as inputs, and the associated missing transverse momentum, taken as the negative vector sum of the $\vec{p_T}$ of those jets.

The effects arising from the detector acceptance, reconstruction efficiency, and selection efficiency, whose combination is referred to as the total reconstruction efficiency, are determined from simulated events. These events are generated with PYTHIA 6.4 [15], the heavy-flavor hadrons are decayed with EVTGEN 1.3.0 [25], and the final-state particles are propagated through a simulation of the CMS detector based on GEANT4 v10.00.p02 [26]. The simulated events used to determine the efficiency demand a $D^{*+}$ meson with $p_T > 3.9\,\text{GeV}$, which is required to decay via $D^{*+} \to D^0 \pi_S^+ \to K^- \pi^+ \pi_S^+$. The $p_T$ threshold does not bias the $p_T$ spectrum for the $D^{*+}$ and $D^0$ events as this measurement is only for D mesons with $p_T > 4\,\text{GeV}$. This sample is also used to determine the $D^+$ efficiency, where the $D^+$ originates from the hadronization of the other charm quark in each event. In this case, the $p_T$ spectrum is biased by the $p_T$ threshold on the $D^{*+}$, and therefore, the simulated $D^+$ $p_T$ distribution is reweighted to match the $D^{*+}$ spectrum. The effects of PU have been included by overlaying generated minimum-bias events with the main simulated collision. The distribution of the number of PU events is reweighted in the simulation to match the

| Variables | $D^{*+}$ | $D^0$ | $D^+$ |
|---|---|---|---|
| Tracks: $p_T$ (GeV) | $> 0.5$ ($> 0.3$ for $\pi_S^+$) | $> 0.8$ | $> 0.7$ |
| Tracks: $\chi^2/$dof | $< 2.5$ ($< 3$ for $\pi_S^+$) | $< 2.5$ | $< 2.5$ |
| Tracks: tracker hits | $\geq 5$ ($\geq 3$ for $\pi_S^+$) | $\geq 5$ | $\geq 5$ |
| Tracks: pixel hits | $\geq 2$ (none for $\pi_S^+$) | $\geq 2$ | $\geq 2$ |
| Tracks: $IP_{xy}$ (cm) | $< 0.1$ ($< 3\sigma$ for $\pi_S^+$) | $< 0.1$ | $< 0.1$ |
| Tracks: $IP_z$ (cm) | $< 1$ ($< 3\sigma$ for $\pi_S^+$) | $< 1$ | $< 1$ |
| $|M_{\mathrm{cand}} - M^{\mathrm{PDG}}|$ (GeV) | $< 0.023$ (for $D^0$) | $< 0.1$ | $< 0.1$ |
| SV fit probability | $> 1\%$ | | |
| Pointing, $\cos\alpha$ | $> 0.99$ | | |
| SV significance | $> 3$ | $> 5$ | $> 10$ |

**Table 1**. The selection requirements for each charm meson.

observed data distribution, separately for the 7 main data-taking periods. Following these corrections, the distributions of the kinematic and selection criteria variables obtained from simulation are found to agree with the data for all three mesons.

## 4 Analysis strategy

### 4.1 Charm meson reconstruction

The first step in the reconstruction of the charm mesons is the selection of tracks corresponding to the final-state objects. The criteria used to select the tracks include a minimum $p_T$, a maximum $\chi^2$ of the track fit divided by the number of degrees of freedom (dof), a minimum number of hits in the pixel detector and in the full tracker (pixel and strip detectors), and maximum impact parameters with respect to the PV in the transverse plane ($IP_{xy}$) and longitudinal direction ($IP_z$). The track requirements are summarized in table 1.

The $D^0$ ($D^+$) mesons are reconstructed by combining two (three) tracks with total charge 0 (1) and having an invariant mass $M_{\mathrm{cand}}$ within 100 MeV of the nominal meson mass $M^{\mathrm{PDG}}$ [27]. When the $D^0$ candidates are reconstructed in the $D^{*+}$ decay chain, a mass window of 23 MeV on the $D^0$ mass is used, instead. In the $p_T$ range relevant for this analysis, charged pions and kaons cannot be identified efficiently in the CMS detector. A kaon or pion mass hypothesis is thus assumed for the tracks, according to the charge and the specific decay channel. Three topological requirements, whose values are given in table 1, are also used to reduce the background, which is primarily from random combinations of tracks. First, the secondary vertex (SV) fit $\chi^2$ probability from fitting the two ($D^0$) or three ($D^+$) tracks to a common vertex is used to ensure the tracks originate from a common point. Second, the cosine of the angle ($\cos\alpha$) between the charm candidate momentum and the vector pointing from the PV to the SV is used to ensure the D meson is consistent with originating from the PV, which reduces background from b hadron decays as well as from random track combinations. Third, the SV significance is the distance between the

PV and SV divided by its uncertainty. This is a crucial requirement in the analysis, which provides a considerable reduction in the combinatorial background that is dominated by tracks originating from the PV.

To complete the $D^{*+}$ meson reconstruction, a third track, corresponding to the slow pion, has a pion mass assigned and is kinematically combined with the $D^0$ candidate. Looser requirements on the $p_T$, $\chi^2/\text{dof}$, and total number of hits are used for this track, as detailed in table 1. In addition, the impact parameter requirements are changed to require that $\text{IP}_{xy}$ and $\text{IP}_z$ be less than three times their respective uncertainties. To improve the mass resolution, the mass difference $\Delta M = m(K\pi\pi_S^+) - m(K\pi)$ is used in the analysis instead of the invariant mass of the three-track combination.

For each event, we require there be no more than one candidate for each of the six decay modes (three mesons and two charge-conjugate states). For events in which there is more than one candidate in a particular decay mode, the candidate whose invariant mass is closest to $M^{PDG}(D)$ [27] is chosen for $D^0$ and $D^+$ candidates and the smallest $\Delta M$ for the $D^{*+}$ candidates. This arbitration is required for 2, 3, and 11% of the events with a $D^{*+}$, $D^0$, and $D^+$ candidate, respectively. By comparing with a random arbitration scheme, it was verified that this method does not introduce a statistically significant bias in terms of the signal yield or signal invariant mass distribution. However, a bias in the background shape has been identified for the $D^+$ mesons, which is described in section 5.

## 4.2 Signal yield determination

The prompt charm meson differential cross section $d\sigma/dp_T$ is measured in 9 bins of $p_T$ between 4 and 100 GeV in the range $|\eta| < 2.1$; the differential cross section $d\sigma/d|\eta|$ is measured in 10 bins of $|\eta|$, for $|\eta| < 2.1$ and $4 < p_T < 100$ GeV.

The signal yields, including both prompt and nonprompt decays, are determined using unbinned maximum-likelihood fits to the invariant mass distributions for the various decay modes (the $\Delta M$ distribution is used for the $D^{*+}$) in each $p_T$ and $|\eta|$ bin. The signal components are modeled by the sum of two Gaussian functions to account for the nonuniform resolution over the detector acceptance. The two Gaussian function means are constrained to be the same. The mean, widths, and normalizations are treated as free parameters. An additional Gaussian function is used to describe the invariant mass shape of $D^0$ candidates with incorrect pion and kaon mass assignments. The width of this wide Gaussian is taken from simulation bin by bin. The normalization of the wide Gaussian function contribution is fixed to be the same as that of the sum of the two narrow signal Gaussian functions in each bin, reflecting the fact that the number of correct and swapped $K/\pi$ $D^0$ signal candidates is the same by construction.

The combinatorial background is described with different functions, according to the decay mode. For the $D^{*+}$ meson, the background is described by a phenomenological threshold function [28] given by

$$f = \left(1 - e^{-\frac{\Delta M - M_0}{p_0}}\right)\left(\frac{\Delta M}{M_0}\right)^{p_1} + p_2\left(\frac{\Delta M}{M_0} - 1\right),$$
(4.1)

| $p_{\mathrm{T}}$ range (GeV) | $\mathrm{D}^{*+}$ | $\mathrm{D}^0$ | $\mathrm{D}^+$ |
|:---:|:---:|:---:|:---:|
| 4–5 | $901 \pm 40$ | $5200 \pm 700$ | $5850 \pm 1400$ |
| 5–6 | $1555 \pm 99$ | $5480 \pm 400$ | $3390 \pm 460$ |
| 6–7 | $1450 \pm 98$ | $5640 \pm 450$ | $3620 \pm 140$ |
| 7–8 | $1144 \pm 75$ | $3990 \pm 500$ | $2790 \pm 130$ |
| 8–12 | $2962 \pm 80$ | $9750 \pm 320$ | $6860 \pm 180$ |
| 12–16 | $1170 \pm 63$ | $3540 \pm 170$ | $3047 \pm 96$ |
| 16–24 | $647 \pm 28$ | $2040 \pm 120$ | $1821 \pm 77$ |
| 24–40 | $180 \pm 15$ | $625 \pm 58$ | $628 \pm 61$ |
| 40–100 | $38 \pm 6$ | $91 \pm 20$ | $83 \pm 11$ |

**Table 2**. The signal yields in data for $\mathrm{D}^{*+}$, $\mathrm{D}^0$, and $\mathrm{D}^+$ mesons in $p_{\mathrm{T}}$ bins for $|\eta| < 2.1$. Only the statistical uncertainties are reported.

where $M_0$ is the endpoint, taken to be the pion mass, and $p_{0,1,2}$ are free parameters. For the $\mathrm{D}^0$ and $\mathrm{D}^+$ mesons, the combinatorial background component is modeled by a third-degree polynomial function, where the four parameters, including the normalization, are unconstrained in the fits.

In figure 1, the fitted invariant mass distributions are reported for two example $p_{\mathrm{T}}$ bins, low (5–6 GeV) and high (16–24 GeV); while figure 2 shows the fitted invariant mass distributions for the bins $|\eta| < 0.2$ and $1.6 < |\eta| < 1.8$. As expected, at low $p_{\mathrm{T}}$ and high $|\eta|$, the track momentum and position resolutions are worse, which affect the reconstructed mass width and the distribution shapes, resulting in an increase in the combinatorial background under the peak. Despite the different kinematic regions, it was found that the same functions with different parameter values reproduce all the distributions well.

The signal yields and the statistical uncertainties returned by the fits are reported in tables 2 and 3 for the $p_{\mathrm{T}}$ and $|\eta|$ bins, respectively.

### 4.3 Efficiency estimation

The efficiency is estimated using the signal MC sample and is defined as the fraction of charm signal decays, generated in the kinematic region $4 < p_{\mathrm{T}} < 100$ GeV and $|\eta| < 2.1$, that is reconstructed and survives the selection criteria described in section 4.1. The efficiency is thus determined for each $p_{\mathrm{T}}$ and $|\eta|$ bin and for both the charge-conjugate states. Taking the $\mathrm{D}^{*+}$ channel as an example, these values range from 0.6% for $4 < p_{\mathrm{T}} < 5$ GeV to 30% for $40 < p_{\mathrm{T}} < 100$ GeV, and from 3.8% for $|\eta| < 0.2$ to 1.5% for $1.8 < |\eta| < 2.1$.

### 4.4 Contamination from nonprompt decays

The aim of this work is to measure the prompt open-charm production cross sections. Thus, it is important to evaluate and subtract the contribution coming from nonprompt charm mesons arising from b hadron decays. Since consistency with the PV is already
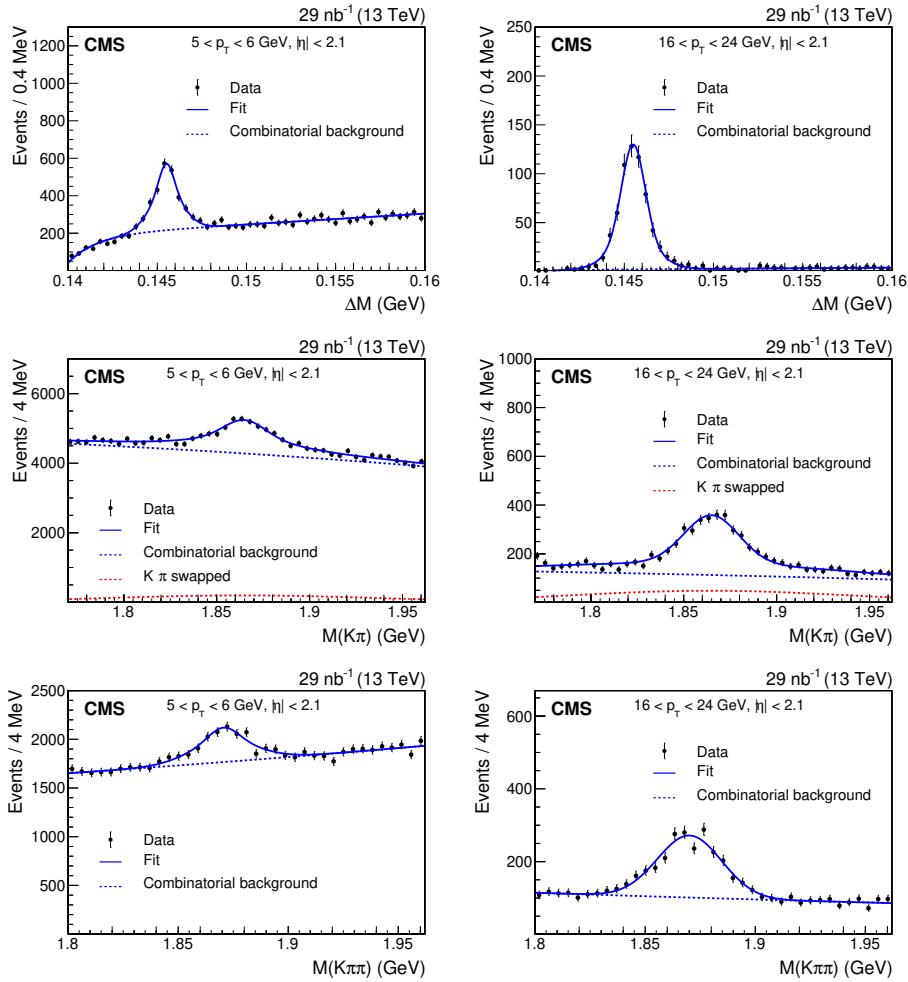
**Figure 1**. The invariant mass distributions: $\Delta M = M(\mathrm{K}^-\pi^+\pi_\mathrm{S}^+) - M(\mathrm{K}^-\pi^+)$ (upper), $M(\mathrm{K}^-\pi^+)$ (middle), and $M(\mathrm{K}^-\pi^+\pi^+)$ (lower); charge conjugation is implied. Plots in the left column show the $5 < p_\mathrm{T} < 6\,\mathrm{GeV}$ bin, while the $16 < p_\mathrm{T} < 24\,\mathrm{GeV}$ bin is shown in the right column. The vertical bars on the points represent the statistical uncertainties in the data. The overall result from the fit is shown by the solid line, the fit to the combinatorial background by the dotted line, and, in the middle plots, the fit to the $\mathrm{K}/\pi$ swapped candidates by the red dot-dashed line.

part of the selection requirements, the prompt signals and secondary-decay components have similar kinematic variable distributions. The nonprompt-background fraction is estimated from simulation, using minimum-bias events generated with the PYTHIA 8 tune CUETP8M1 [29]. From the generator-level information, two subsamples are identified as being representative of the prompt and nonprompt charm meson contributions. The same reconstruction strategy as the one described in section 4.1 is applied to each of them, and the yields are computed following the method for yield evaluation reported in section 4.2, and are labeled $N_\mathrm{prompt}$ and $N_\mathrm{nonprompt}$, respectively. The contamination is then evaluated as the ratio of $N_\mathrm{nonprompt}$ to the sum ($N_\mathrm{prompt} + N_\mathrm{nonprompt}$) for each $p_\mathrm{T}$ and $|\eta|$ bin. The contamination is nonnegligible, ranging from 5 to 17%, depending on the $p_\mathrm{T}$ and $|\eta|$ bin
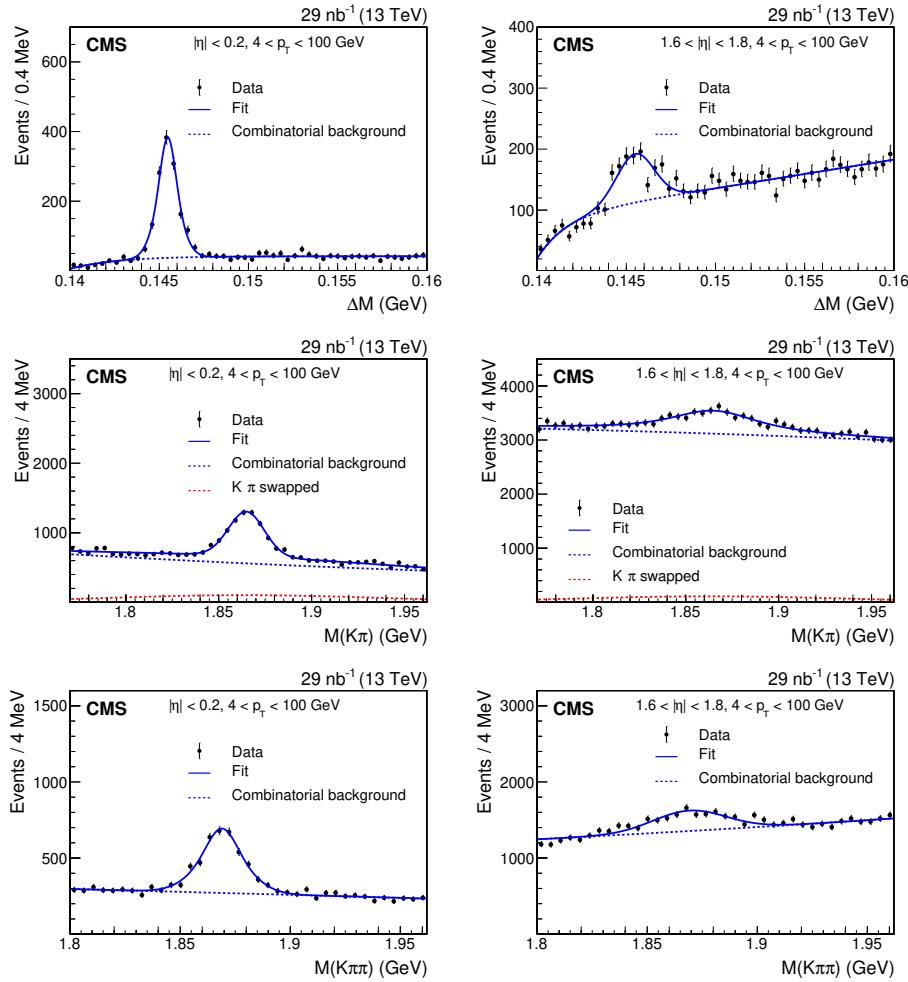
**Figure 2**. The invariant mass distributions: $\Delta M = M(\mathrm{K}^-\pi^+\pi_{\mathrm{S}}^+) - M(\mathrm{K}^-\pi^+)$ (upper), $M(\mathrm{K}^-\pi^+)$ (middle), and $M(\mathrm{K}^-\pi^+\pi^+)$ (lower); charge conjugation is implied. Plots in the left column show the $|\eta| < 0.2$ bin, while the $1.6 < |\eta| < 1.8$ bin is shown in the right column. The vertical bars on the points represent the statistical uncertainties in the data. The overall result from the fit is shown by the solid line, and the fit to the combinatorial background by the dotted line, and, in the middle plots, the fit to the $\mathrm{K}/\pi$ swapped candidates by the red dot-dashed line.

and on the reconstructed meson. This is expected because the requirement on the decay length significance to reject combinatorial backgrounds tends to enhance the contribution from long-lived hadrons. In figure 3, the nonprompt-background fractions for the three mesons are shown as a function of $p_{\mathrm{T}}$ (left) and $|\eta|$ (right).

The fraction of nonprompt events in the signal samples is thus taken from simulation, after ensuring a good description of data events in all the relevant quantities. The fractions are found to be consistent using different generator settings and with CMS measurements at 5 TeV [4, 30], extrapolated to the final states and kinematic region of this measurement. The nonprompt contribution obtained with this method is subtracted from the measured values of the visible event rate for each $p_{\mathrm{T}}$ and $|\eta|$ bin to get the final prompt results.

| $|\eta|$ range | $D^{*+}$ | $D^0$ | $D^+$ |
|---|---|---|---|
| 0–0.2 | $1227 \pm 42$ | $3640 \pm 120$ | $3200 \pm 110$ |
| 0.2–0.4 | $1340 \pm 61$ | $4150 \pm 140$ | $3060 \pm 96$ |
| 0.4–0.6 | $1276 \pm 45$ | $4280 \pm 150$ | $2910 \pm 190$ |
| 0.6–0.8 | $1288 \pm 48$ | $4590 \pm 180$ | $3200 \pm 230$ |
| 0.8–1.0 | $1283 \pm 68$ | $3700 \pm 210$ | $3040 \pm 140$ |
| 1.0–1.2 | $1026 \pm 88$ | $4270 \pm 320$ | $3180 \pm 160$ |
| 1.2–1.4 | $857 \pm 61$ | $3180 \pm 300$ | $2850 \pm 160$ |
| 1.4–1.6 | $576 \pm 59$ | $3050 \pm 320$ | $2350 \pm 250$ |
| 1.6–1.8 | $530 \pm 84$ | $3000 \pm 460$ | $2130 \pm 210$ |
| 1.8–2.1 | $539 \pm 69$ | $3770 \pm 590$ | $2780 \pm 490$ |

**Table 3**. The signal yields in data for $D^{*+}$, $D^0$, and $D^+$ mesons with $4 < p_T < 100 \, \text{GeV}$ in $|\eta|$ bins. Only the statistical uncertainties are reported.
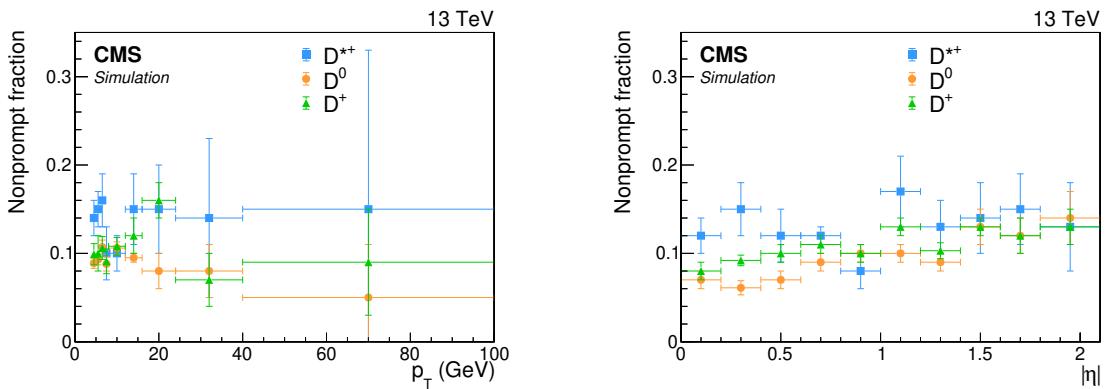


**Figure 3**. The nonprompt fractions found from simulation, as a function of $p_T$ (left) and $|\eta|$ (right) for $D^{*+}$ (squares), $D^0$ (circles), and $D^+$ (triangles) mesons. The vertical lines represent the statistical uncertainties and the horizontal lines the bin widths.

## 5 Systematic uncertainties

Several systematic uncertainty sources are considered in the measurement of the charm meson cross sections. The dominant effects come from the uncertainties related to the tracking efficiency and the modeling of the invariant mass distributions used in the fit for both the signal and background components. The uncertainties considered in this analysis can be organized into three different categories: decay mode and kinematic bin dependent, only decay mode dependent, and independent of both decay mode and bin.

The first category includes the uncertainty in the efficiency coming from the finite number of MC simulation events, resulting in systematic uncertainties of 0.3, 0.3, and 3.5%, respectively, for the $D^{*+}$, $D^0$, and $D^+$ meson cross sections. The last uncertainty is larger than the other two since the sample was enriched in $D^{*+} \to D^0 \pi_S^+ \to K^- \pi^+ \pi_S^+$ decays.

The uncertainties in the nonprompt event contamination have been treated similarly, considering the limited number of events in the MC simulation. The uncertainties in the CMS nonprompt charm measurement [30] and its extrapolation are propagated as an additional uncertainty of 2%, applied to the three mesons. The resulting systematic uncertainties are 3.5, 2.2, and 2.4% for the $D^{*+}$, $D^0$, and $D^+$ cross sections, respectively.

The mass arbitration requirement can produce a peaking background for the small number of events affected by the arbitration, which contributes to the first uncertainty category. This was studied in simulation by selecting a control region that does not contain events with charm mesons and was found to have a nonnegligible contribution only for the $D^+$ meson. The effect for the $D^+$ was evaluated in each bin and found to contribute a systematic uncertainty of 8% for $p_T < 12\,\text{GeV}$, but to be negligible at higher $p_T$ values. This contribution is independent of $|\eta|$, and an uncertainty of 6% is assigned for all $|\eta|$ bins. This is considered as part of the background modeling systematic uncertainty.

Another source of systematic uncertainty that is included in the first category comes from the $p_T$ selection criterion applied to the $\pi_S^+$ in the $D^{*+}$ decay chain. The $p_T$ spectrum of the slow pion peaks below $0.5\,\text{GeV}$ and the selection requirement of $p_T > 0.3\,\text{GeV}$ affects the reconstruction efficiency of the $D^{*+}$ in the first $p_T$ bin (4–5 GeV). A systematic uncertainty of 9% is assigned for this bin, which reflects the variation of the simulated event efficiency calculation in the two $p_T$ bins of the $\pi_S^+$: $0.2 < p_T < 0.3\,\text{GeV}$ and $0.3 < p_T < 0.4\,\text{GeV}$.

Since a reweighting is applied to simulated events in order to reproduce the data PU distribution, a systematic uncertainty is evaluated for each final state. The systematic uncertainty is estimated using the weight calculated for each bin. The cross sections are re-evaluated using the weights raised and lowered by their statistical uncertainties. The largest bin-by-bin change with respect to the cross section calculated with the central value of the weight is taken as the corresponding systematic uncertainty. The total effect is 1% for $D^{*+}$ and $D^0$, and 2% for $D^+$.

The uncertainties associated with the branching fraction values and the track reconstruction efficiency depend on the decay mode but not on the candidate $p_T$ or $|\eta|$. The first one is taken from ref. [27] and has values of 1.1, 0.8, and 1.7% for $D^{*+}$, $D^0$, and $D^+$, respectively. An uncertainty is assigned to the track reconstruction efficiency according to ref. [31]. A different procedure is needed for the slow pion from the $D^{*+}$ decay. Because of the soft $p_T$ spectrum, a lower tracking efficiency is expected. The uncertainty related to the slow pion is computed by comparing the yield in data and MC simulated events when varying the $p_T$ and $|\eta|$ of the slow pion. This results in a systematic uncertainty of 5.2%. Combining the uncertainties for each track, the total systematic uncertainty from the tracking efficiency is 9.4, 4.2, and 6.1% for the $D^{*+}$, $D^0$, and $D^+$ meson cross sections, respectively.

The systematic uncertainty due to the modeling of the invariant mass distribution also falls into the second category. As described in section 4.2, the signal yields are computed by modeling the resonance peaks with a double-Gaussian function in order to take into account the different resolution effects in various kinematic regions. The uncertainty is estimated by using instead a single-Gaussian function, the sum of three Gaussian functions, and a Crystal Ball function [32, 33]. The largest deviation with respect to the default choice is then taken

| Source | D$^{*+}$ | D$^0$ | D$^+$ |
|---|---|---|---|
| Signal efficiency calculation | 0.3 | 0.3 | 3.5 |
| Nonprompt contamination | 3.5 | 2.2 | 2.4 |
| PU reweighting | 1.0 | 1.0 | 2.0 |
| Branching fraction | 1.1 | 0.8 | 1.7 |
| Tracking efficiency | 9.4 | 4.2 | 6.1 |
| Signal modeling | 3.6 | 5.0 | 4.2 |
| Background modeling | 1.2 | 4.8 | 8.0 |
| Integrated luminosity | 2.5 | 2.5 | 2.5 |
| Time-dependent inefficiency | 1.4 | 1.4 | 1.4 |
| Total | 11.2 | 9.0 | 12.3 |

**Table 4**. Summary of the systematic uncertainties (%) in the D$^{*+}$, D$^0$, and D$^+$ meson cross sections. For the bin-dependent systematic uncertainties in the table, the weighted average is shown. The total uncertainty is the sum in quadrature of the individual contributions.

as the systematic uncertainty, yielding 3.6, 5.0, and 4.2% for the D$^{*+}$, D$^0$, and D$^+$ meson cross sections, respectively. For the combinatorial background description, the systematic uncertainty is evaluated by replacing the baseline function with a fourth-degree polynomial, resulting in 1.2, 4.8, and 5.3% for the D$^{*+}$, D$^0$, and D$^+$ meson cross sections, respectively.

The last category, containing uncertainties independent of both decay modes and kinematic variables, includes those due to data-taking conditions and variation in detector performance. The systematic uncertainty in the integrated luminosity for 2016 is 2.5% [34]. During the 2016 run, the CMS tracker suffered some time-dependent inefficiencies that resulted in a nonnegligible change in charm meson yields. The average PU rate also varied during the data taking. Both these effects are taken into account by correcting the different runs for the tracker inefficiency, which was determined from simulation after the PU distribution in the simulated events was reweighted to match the data. The resulting systematic uncertainty in the correction is estimated to be 1.4%.

All the systematic uncertainties, except the one applied only to the first $p_{\mathrm{T}}$ bin of the D$^{*+}$, are summarized in table 4. For the bin-dependent systematic uncertainties, the value given in table 4 is an average that is weighted by the number of signal events. The total uncertainty is evaluated as the sum in quadrature of the individual contributions.

| | $\mathrm{d}\sigma/\mathrm{d}p_{\mathrm{T}}$ ($\mu$b/GeV) | | |
|---|---|---|---|
| $p_{\mathrm{T}}$ bin [GeV] | $\mathrm{D}^{*+} + \mathrm{D}^{*-}$ | $\mathrm{D}^0 + \overline{\mathrm{D}}^0$ | $\mathrm{D}^+ + \mathrm{D}^-$ |
| 4–5 | $166 \pm\ 7\ \pm 24$ | $430 \pm\ 58\ \pm 38$ | $250 \pm\ 61\ \pm 34$ |
| 5–6 | $96 \pm\ 6\ \pm 11$ | $230 \pm\ 17\ \pm 21$ | $79 \pm\ 11\ \pm 11$ |
| 6–7 | $47 \pm\ 3\ \pm 5$ | $136 \pm\ 11\ \pm 12$ | $50 \pm\ 2\ \pm 7$ |
| 7–8 | $25.6 \pm 1.7 \pm 2.9$ | $66 \pm\ 8\ \pm 6$ | $29.5 \pm 1.4 \pm 4.3$ |
| 8–12 | $8.8 \pm 0.2 \pm 1.0$ | $21.0 \pm 0.7 \pm 1.9$ | $9.4 \pm 0.3 \pm 1.2$ |
| 12–16 | $1.70 \pm 0.09 \pm 0.20$ | $3.93 \pm 0.19 \pm 0.44$ | $2.05 \pm 0.07 \pm 0.24$ |
| 16–24 | $(3.52 \pm 0.15 \pm 0.42) \times 10^{-1}$ | $(8.1 \pm 0.5 \pm 0.9) \times 10^{-1}$ | $(4.06 \pm 0.17 \pm 0.51) \times 10^{-1}$ |
| 24–40 | $(4.1 \pm 0.3 \pm 0.6) \times 10^{-2}$ | $(9.7 \pm 0.9 \pm 1.3) \times 10^{-2}$ | $(6.0 \pm 0.6 \pm 1.0) \times 10^{-2}$ |
| 40–100 | $(2.3 \pm 0.4 \pm 0.5) \times 10^{-3}$ | $(3.3 \pm 0.7 \pm 0.8) \times 10^{-3}$ | $(2.3 \pm 0.3 \pm 1.7) \times 10^{-3}$ |

**Table 5**. The differential cross sections of prompt $\mathrm{D}^{*+} + \mathrm{D}^{*-}$, $\mathrm{D}^0 + \overline{\mathrm{D}}^0$, and $\mathrm{D}^+ + \mathrm{D}^-$ production in $p_{\mathrm{T}}$ bins with $|\eta| < 2.1$; the first uncertainty is statistical, the second is systematic.

## 6 Results

The differential cross sections for prompt charm meson production as a function of $p_{\mathrm{T}}$ and $|\eta|$ are determined using the equations:

$$\frac{\mathrm{d}\sigma(\mathrm{pp} \to \mathrm{D}X)}{\mathrm{d}p_{\mathrm{T}}} = \frac{N_i(\mathrm{D} \to f)}{\Delta p_{\mathrm{T}i}\, \mathcal{B}(\mathrm{D} \to f)\, \mathcal{L}\, \varepsilon_i(\mathrm{D} \to f)}\,, \tag{6.1}$$

$$\frac{\mathrm{d}\sigma(\mathrm{pp} \to \mathrm{D}X)}{\mathrm{d}|\eta|} = \frac{N_i(\mathrm{D} \to f)}{\Delta \eta_i\, \mathcal{B}(\mathrm{D} \to f)\, \mathcal{L}\, \varepsilon_i(\mathrm{D} \to f)}\,, \tag{6.2}$$

where $N_i(\mathrm{D} \to f)$ is the number of prompt charm mesons reconstructed in the selected final state $f$ (including the charge-conjugate final state) for each bin i, after subtracting the non-prompt backgrounds, $\Delta p_{\mathrm{T}}$ and $\Delta \eta = 2\Delta|\eta|$ are the bin widths, $\mathcal{B}(\mathrm{D} \to f)$ is the branching fraction of the reconstructed decay, $\varepsilon_i(\mathrm{D} \to f)$ is the total reconstruction efficiency of the decay chain evaluated using simulated events, and $\mathcal{L}$ is the integrated luminosity.

In tables 5 and 6, the differential cross section values and their uncertainties are reported for each $p_{\mathrm{T}}$ and $|\eta|$ bin, respectively. The first uncertainty is statistical and the second is systematic. The latter is the dominant one in the majority of the $p_{\mathrm{T}}$ and $|\eta|$ bins.

The differential cross sections for the three charm mesons, as a function of $p_{\mathrm{T}}$ (upper) and $|\eta|$ (lower), are shown in figures 4–6, where the data points are compared to several MC predictions and theoretical calculations. The cross section values are compared to:

- the predictions at next-to-leading-order (NLO) plus next-to-leading-logarithmic accuracy from FONLL [17, 18] calculations, shown as bands representing the upper and lower limits for a given $p_{\mathrm{T}}$ bin, as detailed below. The parton distribution function (PDF) CTEQ6.6 has been used. The renormalization ($\mu_{\mathrm{R}}$) and factorization ($\mu_{\mathrm{F}}$) scales are set to $\mu_{\mathrm{R}} = \mu_{\mathrm{F}} = \mu_0$ where $\mu_0$ is defined as $\mu_0^2 = m_{\mathrm{c}}^2 + p_{\mathrm{T_c}}^2$ and $m_{\mathrm{c}} = 1.5\,\mathrm{GeV}$ and $p_{\mathrm{T_c}}$ are the mass and transverse momentum of the charm quark, respectively. No default fragmentation fractions are provided for the heavy-hadron

| $\lvert\eta\rvert$ range | $\mathrm{d}\sigma/\mathrm{d}\lvert\eta\rvert$ ($\mu$b) | | |
|---|---|---|---|
| | $\mathrm{D}^{*+} + \mathrm{D}^{*-}$ | $\mathrm{D}^0 + \overline{\mathrm{D}}^0$ | $\mathrm{D}^+ + \mathrm{D}^-$ |
| 0–0.2 | $92 \pm\ 3\ \pm 10$ | $210 \pm\ 7\ \pm 19$ | $87 \pm\ 3\ \pm 11$ |
| 0.2–0.4 | $96 \pm\ 4\ \pm 11$ | $240 \pm\ 8\ \pm 21$ | $90 \pm\ 3\ \pm 12$ |
| 0.4–0.6 | $94 \pm\ 3\ \pm 11$ | $243 \pm\ 9\ \pm 22$ | $86 \pm\ 6\ \pm 11$ |
| 0.6–0.8 | $96 \pm\ 4\ \pm 11$ | $255 \pm 10 \pm 23$ | $93 \pm\ 7\ \pm 12$ |
| 0.8–1.0 | $111 \pm\ 6\ \pm 12$ | $220 \pm 13 \pm 20$ | $102 \pm\ 5\ \pm 19$ |
| 1.0–1.2 | $97 \pm\ 8\ \pm 11$ | $265 \pm 20 \pm 24$ | $107 \pm\ 5\ \pm 20$ |
| 1.2–1.4 | $106 \pm\ 8\ \pm 12$ | $250 \pm 24 \pm 23$ | $106 \pm\ 6\ \pm 29$ |
| 1.4–1.6 | $81 \pm\ 8\ \pm 9$ | $265 \pm 27 \pm 24$ | $109 \pm 12 \pm 28$ |
| 1.6–1.8 | $85 \pm 13 \pm 10$ | $298 \pm 45 \pm 27$ | $112 \pm 11 \pm 24$ |
| 1.8–2.1 | $70 \pm\ 9\ \pm 17$ | $291 \pm 45 \pm 64$ | $123 \pm 22 \pm 27$ |

**Table 6**. The differential cross sections of prompt $\mathrm{D}^{*+} + \mathrm{D}^{*-}$, $\mathrm{D}^0 + \overline{\mathrm{D}}^0$, and $\mathrm{D}^+ + \mathrm{D}^-$ production in $\lvert\eta\rvert$ bins with $4 < p_{\mathrm{T}} < 100\,\mathrm{GeV}$; the first uncertainty is statistical, the second is systematic.

fragmentation; the fragmentation fractions used are 0.243, 0.609, and 0.240 for the $\mathrm{D}^{*+}$, $\mathrm{D}^0$, and $\mathrm{D}^+$, respectively [35]. The parameter variations used for the evaluation of the uncertainty bands are (all variations are added in quadrature):

- scale uncertainties: $\mu_0/2 < \mu_{\mathrm{R}}$, $\mu_{\mathrm{F}} < 2\mu_0$ with $1/2 < \mu_{\mathrm{R}}/\mu_{\mathrm{F}} < 2$;

- charm mass variation: $m_{\mathrm{c}} = 1.3$–$1.7\,\mathrm{GeV}$;

- PDF uncertainties: calculated according to the individual PDF set recipe.

Here the universality of charm fragmentation is implicitly still assumed, although recent results in a different kinematic range seem to demonstrate that universality is violated in a $p_{\mathrm{T}}$-dependent way [36–40]. This might in principle require an evaluation of $p_{\mathrm{T}}$-dependent downward corrections to the predicted D meson yields of order 5-20% in the $p_{\mathrm{T}}$ range measured here, while the measurements are not affected. Since a scheme to consistently evaluate and apply such corrections to the FONLL predictions does not yet exist, and the difference is still expected to be subdominant in particular compared to the large QCD scale uncertainties, no uncertainties were assigned for this source here.

- leading-order (LO) plus parton shower (PS) simulations using PYTHIA 6.4 [15] with the tune Z2* [41], which is based on the CMS Z1 tune [42], but adopting the CTEQ6L PDF set instead of the previous CTEQ5L. The tune is the result of optimizing two parameters that refer to the regularization scale: $p_{\mathrm{T}\perp 0}$, for multiple interactions at a reference energy and the power exponent of the energy rescaling used to determine the value of $p_{\mathrm{T}\perp 0}$ as it goes to zero at scales different from the reference scale;

- LO plus PS simulations by PYTHIA 8.202 [16] with the tunes:

  - A2, which is an ATLAS minimum-bias tune [43] validated using their kinematic distributions and based on the tune 4C [44], using the MSTW PDF;

  - Monash [45], which was developed by re-evaluating the constraints imposed by LEP and SLD on hadronization, in particular with regard to heavy-quark fragmentation and strangeness production; it is a PYTHIA 8 tune using the NNPDF2.3 LO PDF.

  - CUETP8M1 [29], which is a CMS-specific tune and stands for "CMS Underlying Event Tune PYTHIA 8". It is based on Monash (M1), but the two multiple-parton-interaction (MPI), energy-dependent parameters, which are the MPI cut-off value and the exponent $\epsilon$ of the $\sqrt{s}$ dependence, are determined by fitting underlying events in CMS data at $\sqrt{s} = 0.9$, 1.96, and 7 TeV. In ref. [46] it was shown that neither the Monash nor the CUETP8M1 tunes describe well the central value of underlying events in data at $\sqrt{s} = 13$ TeV. This suggests that the tune CUETP8M1 does not produce enough charged particles at 13 TeV.

The PYTHIA predictions are from samples of various sizes with corresponding varying statistical uncertainties, which are not shown in the figures. The lower panels in figures 4–6 display the ratio of the FONLL and PYTHIA predictions to the data, for which the statistical and total uncertainties are shown by the inner and outer bars, respectively.

The agreement with the different predictions is fair in the wide kinematic range analyzed. However, none of the MC event generators models the data well over the entire measurement region. The measurements tend to favor a higher cross section than predicted by FONLL and a lower one than estimated by PYTHIA, although the predictions from the PYTHIA generator are sensitive to the different tunes used. The cross section predictions from the different PYTHIA tunes differ in both normalization and shape, which confirms that the description of the data provided by the models is sensitive to further model improvements. Overall, the best description of the data is given by the upper edge of the FONLL uncertainty band.

### 6.1 Comparison with other experiments

While there are several previous LHC measurements of charm meson production cross sections, none of them cover the same kinematic region at the same center-of-mass energy as the results presented here. However, since the previous measurements can also be compared to FONLL predictions, it is useful to see if a consistent picture emerges. In the comparisons that follow, no scaling is performed on the previous measurements to account for different kinematic regions, center-of-mass energies, or cross section definitions, but the FONLL predictions were adjusted to match the conditions of the various results.

The measurements from the ATLAS experiment [5], although performed with data collected at $\sqrt{s} = 7$ TeV, are the closest to the ones presented in this paper in terms of the acceptance and kinematic regime. Figure 7 shows both the ATLAS and CMS results, compared to the respective FONLL predictions at $\sqrt{s} = 7$ and 13 TeV for both D$^{*+}$
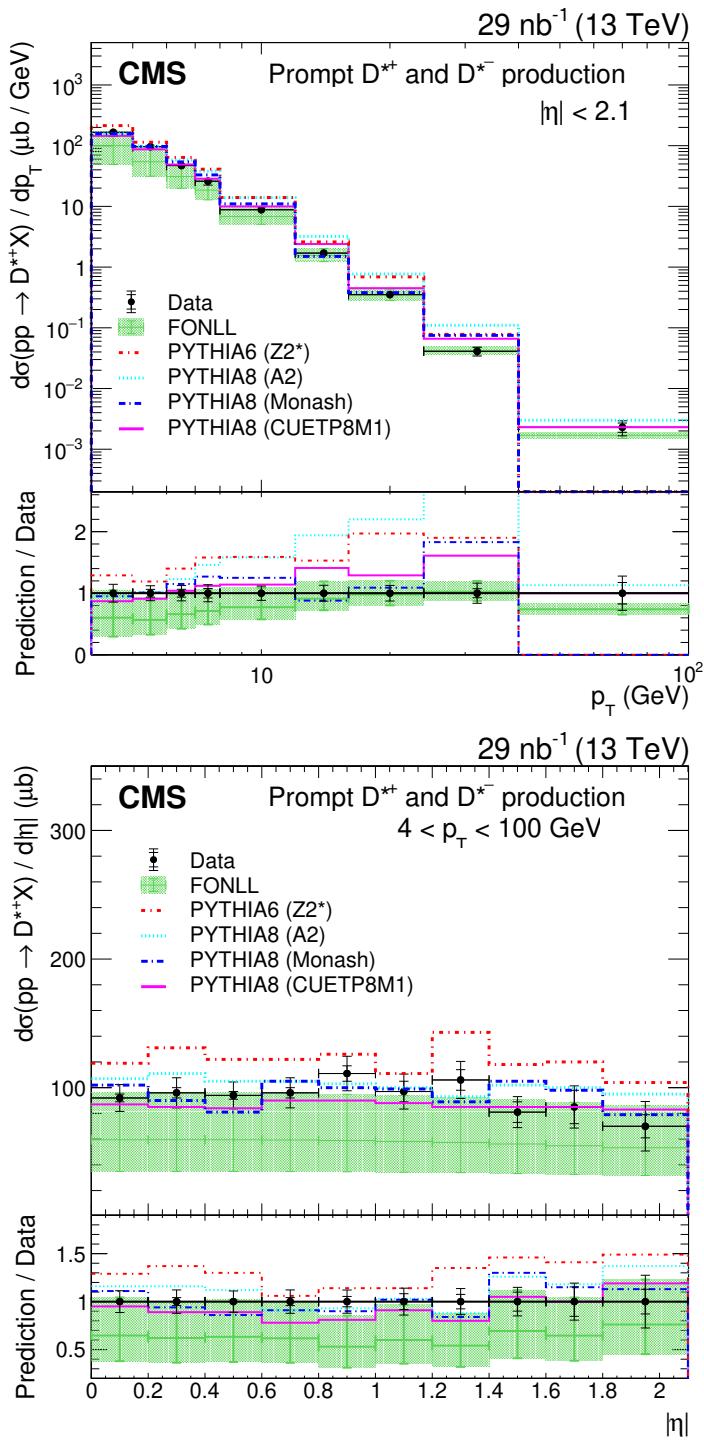
**Figure 4**. Differential cross sections $d\sigma/dp_T$ (upper) and $d\sigma/d|\eta|$ (lower) for prompt $D^{*\pm}$ meson production. Black markers represent the data and are compared with several MC simulation models and theoretical predictions. The statistical and total uncertainties are shown by the inner and outer vertical lines, respectively. The FONLL band represents the standard uncertainties in the prediction as detailed in the text. The lower panel gives the ratios of the predictions to the data.
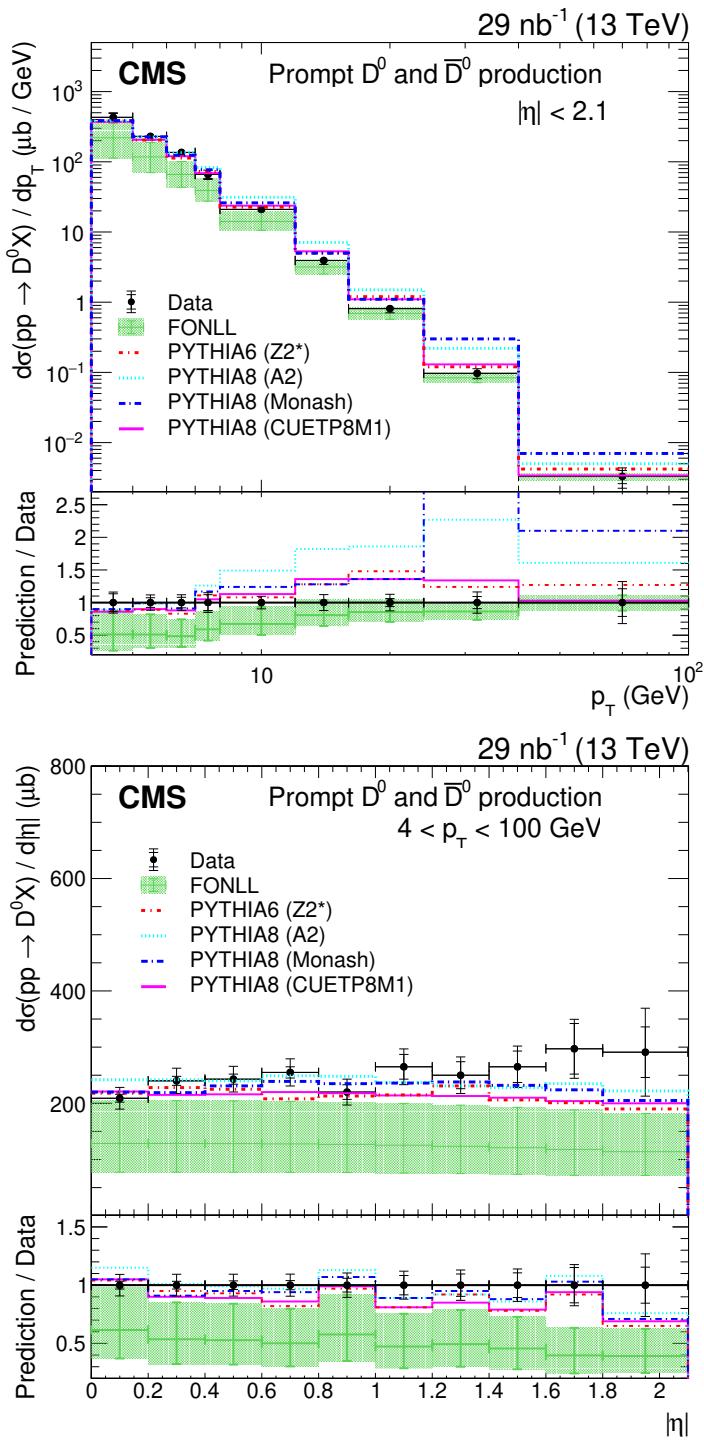
**Figure 5**. Differential cross section $d\sigma/dp_T$ (upper) and $d\sigma/d|\eta|$ (lower) for prompt $D^0$ ($\overline{D}^0$) meson production. Black markers represent the data and are compared with several MC simulation models and theoretical predictions. The statistical and total uncertainties are shown by the inner and outer vertical lines, respectively. The FONLL band represents the standard uncertainties in the prediction as detailed in the text. The lower panel gives the ratios of the predictions to the data.
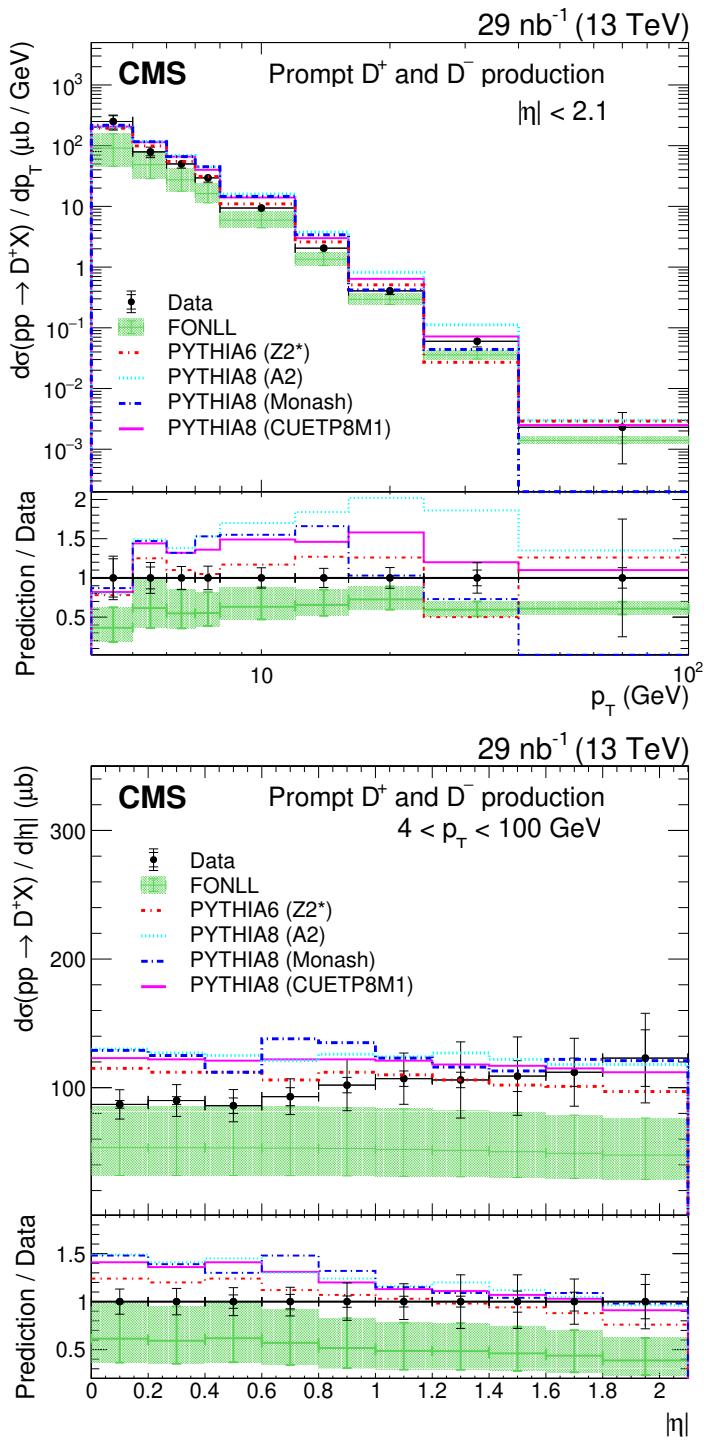
**Figure 6**. Differential cross section $d\sigma/dp_T$ (upper) and $d\sigma/d|\eta|$ (lower) for prompt $D^{\pm}$ meson production. Black markers represent the data and are compared with several MC simulation models and theoretical predictions. The statistical and total uncertainties are shown by the inner and outer vertical lines, respectively. The FONLL band represents the standard uncertainties in the prediction as detailed in the text. The lower panel gives the ratios of the predictions to the data.
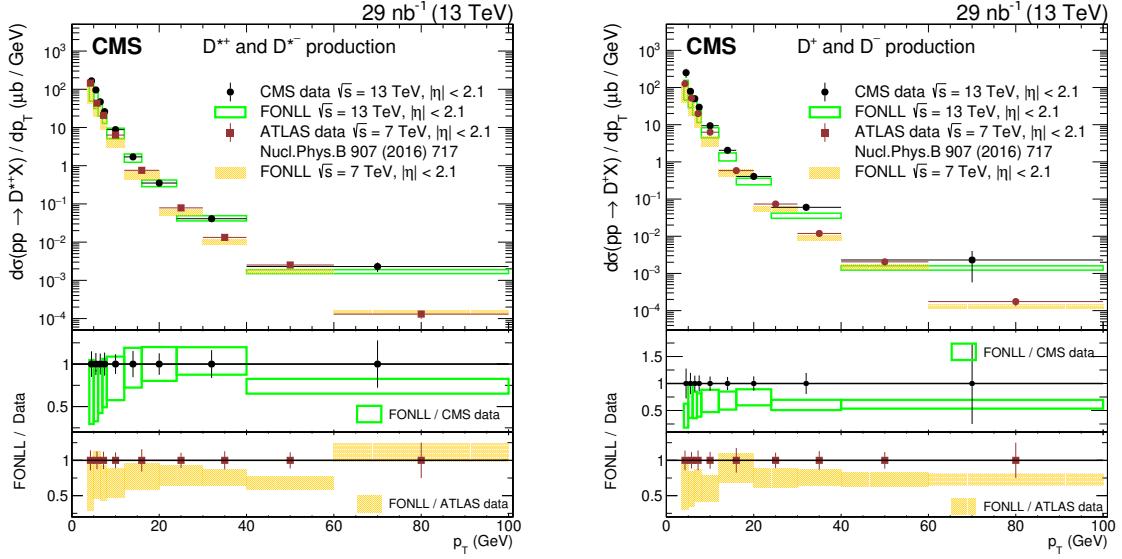
**Figure 7**. Differential cross section $d\sigma/dp_T$ for $D^{*\pm}$ (left) and $D^\pm$ (right) meson production, comparing the production from CMS (black circles, prompt, this paper) at $\sqrt{s} = 13\,\text{TeV}$ and ATLAS (red squares, prompt + nonprompt) at $\sqrt{s} = 7\,\text{TeV}$ [5]. The corresponding predictions from FONLL are shown by the unfilled and filled boxes, respectively. The vertical lines on the points give the total uncertainties in the data, and the horizontal lines show the bin widths. The two lower panels in each plot give the ratios of the FONLL predictions to the CMS and ATLAS data, shown by circles and squares, respectively.

(left) and $D^\pm$ (right) mesons. Since the ATLAS measurement includes both prompt and nonprompt charm mesons, the corresponding FONLL predictions include both components as well. The lower two panels in the figure give the ratio of the FONLL predictions to the respective measurements. The results show good agreement in terms of shape, and the comparison between the data and the theoretical predictions is very similar for the two experiments. The central value of the FONLL predictions tends to underestimate the data, but the upper edge of the FONLL band agrees reasonably well.

Figure 8 shows the comparison with the ALICE results [8, 9] for the $D^{*+}$, $D^0$, and $D^+$ cross sections at $\sqrt{s} = 7\,\text{TeV}$ in the range $1 < p_T < 24\,\text{GeV}$ ($0 < p_T < 36\,\text{GeV}$ for the $D^0$) and for the rapidity region $|y| < 0.5$. Between the two ALICE measurements, the more recent one [9] is chosen for the comparison. It should be noted that the cross section definition by ALICE includes a factor of $1/2$ that accounts for the fact that the measured yields include particles and antiparticles, while the cross sections are given for particles only. The same is true for the corresponding FONLL predictions, as well. To provide a relevant comparison, the CMS measurements are given for $p_T < 24\,\text{GeV}$ ($p_T < 40\,\text{GeV}$ for the $D^0$), for a better comparison with the ALICE points. Both sets of results are consistent with the respective FONLL predictions and close to their upper edge, as shown in the lower two panels.

The CMS experiment has also measured the $D^0$ cross section in pp collisions at $\sqrt{s} = 5.02\,\text{TeV}$ for $|y| < 1$ [4]. Figure 9 shows this measurements in comparison with the FONLL predictions and the corresponding 13 TeV results from this analysis. The rise in cross
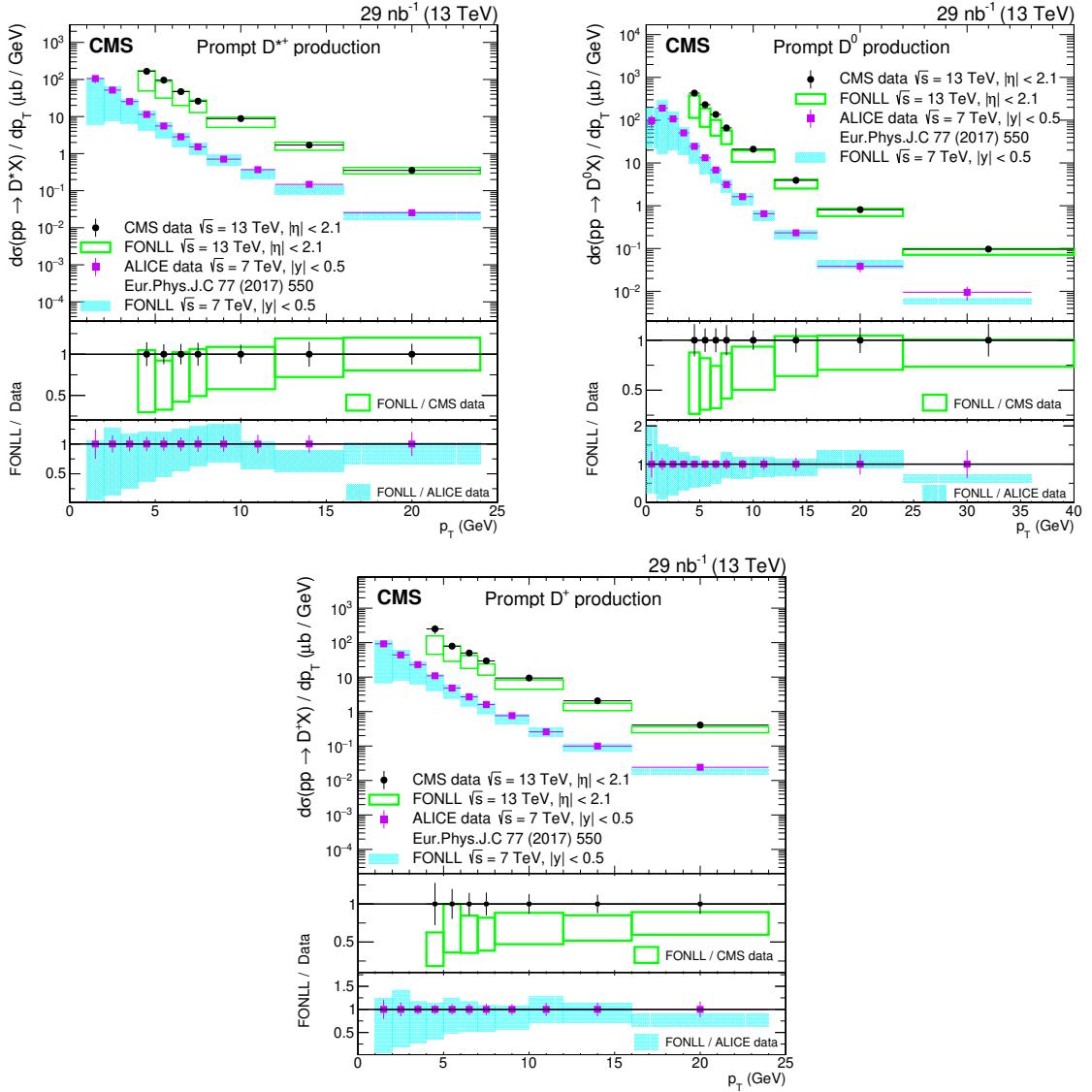
**Figure 8**. Differential cross section $d\sigma/dp_T$ for prompt $D^{*\pm}$ (upper left), $D^0 + \overline{D}^0$ (upper right) and $D^\pm$ (lower) meson production with $p_T < 24$ GeV from CMS (black circles, this paper) at $\sqrt{s} = 13$ TeV and ALICE [9] (magenta squares) at $\sqrt{s} = 7$ TeV and $|y| < 0.5$. The corresponding predictions from FONLL are shown by the unfilled and filled boxes, respectively. The cross section definition by ALICE includes a factor of 1/2 that accounts for the fact that the measured yields include particles and antiparticles while the cross sections are given for particles only. The same is true for the corresponding FONLL predictions, as well. The vertical lines on the points give the total uncertainties in the data, and the horizontal lines show the bin widths. The two lower panels in each plot give the ratios of the FONLL predictions to the CMS and ALICE data, shown by circles and squares, respectively.
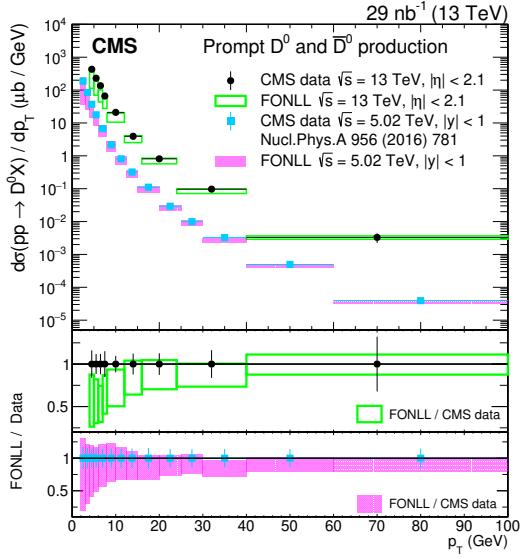
**Figure 9**. Differential cross section $d\sigma/dp_T$ for the prompt $D^0 + \overline{D}^0$ meson production from CMS at $\sqrt{s} = 13\,\text{TeV}$ (black circles, this paper) and $5.02\,\text{TeV}$ [4] (light blue squares) for $|y| < 1$. The corresponding FONLL predictions are shown by the unfilled and filled boxes, respectively. The vertical lines on the points give the total uncertainty in the data, and the horizontal lines show the bin widths. The two lower panels give the ratios of the FONLL predictions to the CMS data at $\sqrt{s} = 13\,\text{TeV}$ and $5.02\,\text{TeV}$, shown by circles and squares, respectively.

section between 5.02 and 13 TeV is obvious from the figure, as well as a similar agreement between the 5.02 TeV measurements and the FONLL predictions.

The only other measurement performed at $\sqrt{s} = 13\,\text{TeV}$ for which the results are publicly available numerically (the results of [10] are only available in the figures) at $\sqrt{s} = 13\,\text{TeV}$ comes from the LHCb Collaboration [13]. Since the $\eta$ acceptances of the CMS and LHCb experiments differ, the two measurements are complementary and the results presented in this paper extend the reconstruction to a rapidity region not covered by LHCb. The two measurements are compared in figure 10 for the LHCb rapidity bin closest to the CMS fiducial region, together with the FONLL predictions. The CMS measurements are shown for $p_T < 16\,\text{GeV}$ to allow a better comparison with the LHCb results. Again, both sets of measurements are in reasonable agreement with the FONLL predictions.
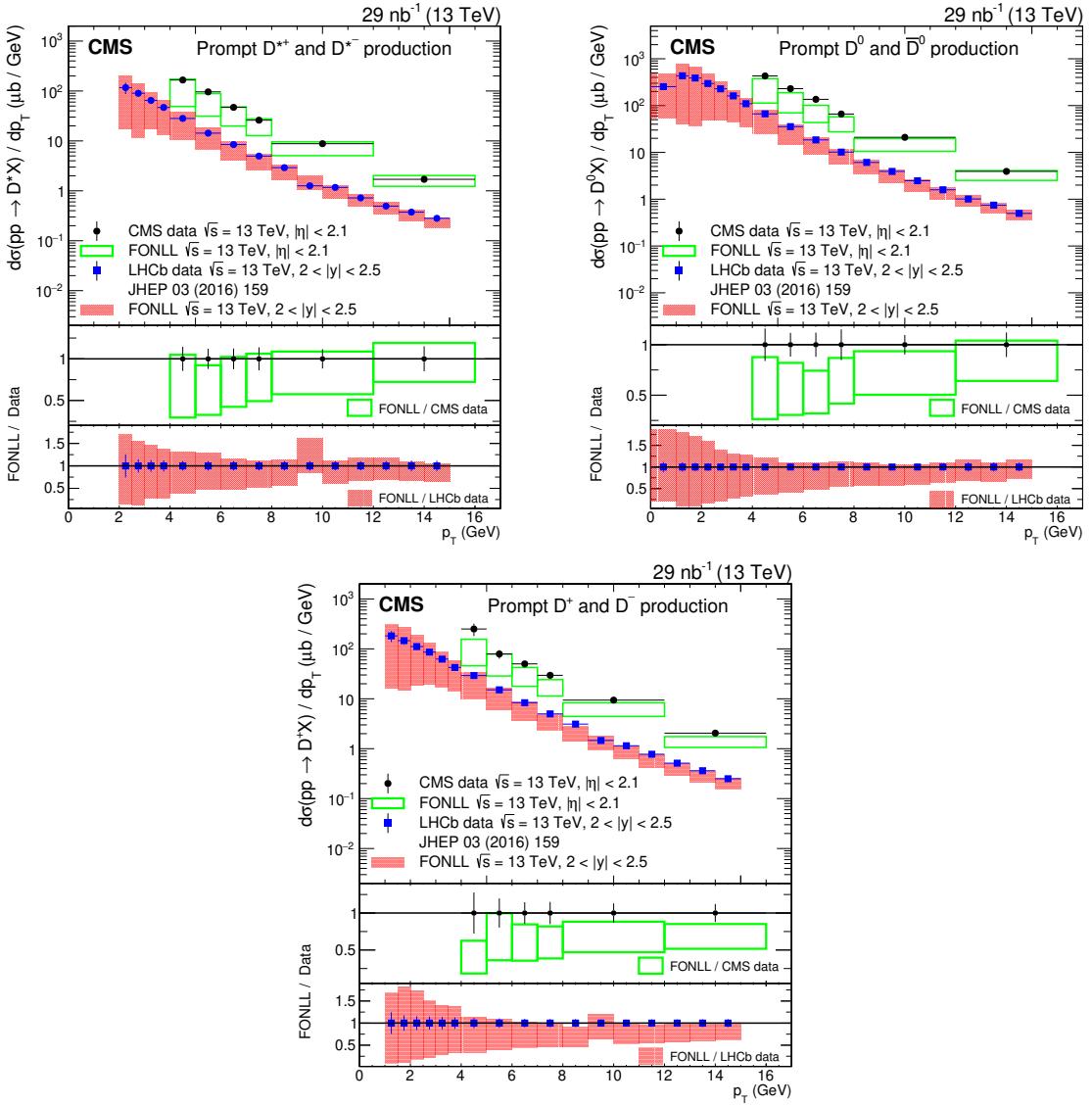
**Figure 10**. Differential cross section $d\sigma/dp_T$ for prompt $D^{*\pm}$ (upper left), $D^0 + \overline{D}^0$ (upper right) and $D^\pm$ (lower) meson production at $\sqrt{s} = 13$ TeV with $p_T < 16$ GeV for CMS (black circles, this paper) for $|\eta| < 2.1$ and LHCb [13] (blue squares) for $2 < |y| < 2.5$. The corresponding FONLL predictions are shown by the unfilled and filled boxes, respectively. To simplify the results representation, the equivalence between $d\sigma/dp_T$ for $2 < |y| < 2.5$ and $d^2\sigma/dp_T dy$ for $2 < y < 2.5$, as in the original publication, has been used. The vertical lines on the points give the total uncertainty in the data, and the horizontal lines show the bin widths. The two lower panels in each plot give the ratios of the FONLL predictions to the CMS and LHCb data, shown by circles and squares, respectively.

# 7  Summary

The differential cross sections $\mathrm{d}\sigma/\mathrm{d}p_\mathrm{T}$ and $\mathrm{d}\sigma/\mathrm{d}|\eta|$ for prompt charm meson ($\mathrm{D}^{*\pm}$, $\mathrm{D}^0$ ($\overline{\mathrm{D}}^0$), and $\mathrm{D}^\pm$) production are measured in the transverse momentum range $4 < p_\mathrm{T} < 100\,\mathrm{GeV}$ and pseudorapidity $|\eta| < 2.1$, using data collected by the CMS experiment in proton-proton collisions in 2016 at $\sqrt{s} = 13\,\mathrm{TeV}$, corresponding to an integrated luminosity of $29\,\mathrm{nb}^{-1}$. The charm mesons were identified with signal invariant mass peaks of high statistical significance. The contamination arising from nonprompt D mesons originating from b hadron decays was removed using Monte Carlo event simulations, validated by measurements.

The measured cross section values are compared to predictions from a theoretical calculation and several different Monte Carlo generators. The agreement with the various models can be considered fair, but no single Monte Carlo simulation or theoretical prediction describes the data well over the entire kinematic range. The measurements tend to favor a higher cross section than predicted by the FONLL calculations [17, 18] and lower than estimated by the PYTHIA event generators [15, 16]. The cross section predictions from the different PYTHIA tunes differ in both normalization and shape, which confirms that the description of the data provided by the models is sensitive to further model improvements. Overall, the best description is obtained by the upper edge of the FONLL uncertainty band, which could be taken as a reference prediction for background estimations for other processes, over the full kinematic range covered by all the LHC measurements. By confirming this finding in kinematic regions not previously covered, this measurement makes a contribution to the understanding of charm meson production in hadronic collisions, which is still dominated by large uncertainties in the present theoretical models.

## Acknowledgments

# References

[1] FASER collaboration, *Technical proposal: FASERnu*, [arXiv:2001.03073](#) [[INSPIRE](#)].

[2] S. Alekhin et al., *A facility to Search for Hidden Particles at the CERN SPS: the SHiP physics case*, [*Rept. Prog. Phys.* **79** (2016) 124201](#) [[arXiv:1504.04855](#)] [[INSPIRE](#)].

[3] C. Ahdida et al., *SND@LHC — Scattering and Neutrino Detector at the LHC*, Tech. Rep. [CERN-LHCC-2021-003](#), CERN, Geneva, Switzerland (2021).

[4] CMS collaboration, *Nuclear modification factor of $D^0$ mesons in PbPb collisions at $\sqrt{s_{\mathrm{NN}}} = 5.02$ TeV*, *Phys. Lett. B* **782** (2018) 474 [arXiv:1708.04962] [ɪɴSPIRE].

[5] ATLAS collaboration, *Measurement of $D^{*\pm}$, $D^{\pm}$ and $D_s^{\pm}$ meson production cross sections in pp collisions at $\sqrt{s} = 7$ TeV with the ATLAS detector*, *Nucl. Phys. B* **907** (2016) 717 [arXiv:1512.02913] [ɪɴSPIRE].

[6] ALICE collaboration, *Measurement of $D^0$, $D^+$, $D^{*+}$ and $D_s^+$ production in pp collisions at $\sqrt{s} = 5.02$ TeV with ALICE*, *Eur. Phys. J. C* **79** (2019) 388 [arXiv:1901.07979] [ɪɴSPIRE].

[7] ALICE collaboration, *Measurement of beauty and charm production in pp collisions at $\sqrt{s} = 5.02$ TeV via non-prompt and prompt D mesons*, *JHEP* **05** (2021) 220 [arXiv:2102.13601] [ɪɴSPIRE].

[8] ALICE collaboration, *Measurement of charm production at central rapidity in proton-proton collisions at $\sqrt{s} = 7$ TeV*, *JHEP* **01** (2012) 128 [arXiv:1111.1553] [ɪɴSPIRE].

[9] ALICE collaboration, *Measurement of D-meson production at mid-rapidity in pp collisions at $\sqrt{s} = 7$ TeV*, *Eur. Phys. J. C* **77** (2017) 550 [arXiv:1702.00766] [ɪɴSPIRE].

[10] ALICE collaboration, *Measurement of prompt $D^0$, $\Lambda_c^+$, and $\Sigma_c^{0,++}(2455)$ production in pp collisions at $\sqrt{s} = 13$ TeV*, arXiv:2106.08278 [ɪɴSPIRE].

[11] LHCb collaboration, *Measurements of prompt charm production cross-sections in pp collisions at $\sqrt{s} = 5$ TeV*, *JHEP* **06** (2017) 147 [arXiv:1610.02230] [ɪɴSPIRE].

[12] LHCb collaboration, *Prompt charm production in pp collisions at $\sqrt{s} = 7$ TeV*, *Nucl. Phys. B* **871** (2013) 1 [arXiv:1302.2864] [ɪɴSPIRE].

[13] LHCb collaboration, *Measurements of prompt charm production cross-sections in pp collisions at $\sqrt{s} = 13$ TeV*, *JHEP* **03** (2016) 159 [*Erratum ibid.* **09** (2016) 013] [*Erratum ibid.* **05** (2017) 074] [arXiv:1510.01707] [ɪɴSPIRE].

[14] *HEPData record for this analysis*, CMS-PAS-BPH-18-003, (2020).

[15] T. Sjöstrand, S. Mrenna and P.Z. Skands, *PYTHIA 6.4 physics and manual*, *JHEP* **05** (2006) 026 [hep-ph/0603175] [ɪɴSPIRE].

[16] T. Sjöstrand et al., *An introduction to PYTHIA 8.2*, *Comput. Phys. Commun.* **191** (2015) 159 [arXiv:1410.3012] [ɪɴSPIRE].

[17] M. Cacciari, M. Greco and P. Nason, *The $p_T$ spectrum in heavy flavor hadroproduction*, *JHEP* **05** (1998) 007 [hep-ph/9803400] [ɪɴSPIRE].

[18] M. Cacciari, M.L. Mangano and P. Nason, *Gluon PDF constraints from the ratio of forward heavy-quark production at the LHC at $\sqrt{s} = 7$ and 13 TeV*, *Eur. Phys. J. C* **75** (2015) 610 [arXiv:1507.06197] [ɪɴSPIRE].

[19] CMS collaboration, *Description and performance of track and primary-vertex reconstruction with the CMS tracker*, 2014 *JINST* **9** P10009 [arXiv:1405.6569] [ɪɴSPIRE].

[20] CMS collaboration, *The CMS trigger system*, 2017 *JINST* **12** P01020 [arXiv:1609.02366] [ɪɴSPIRE].

[21] CMS collaboration, *The CMS experiment at the CERN LHC*, 2008 *JINST* **3** S08004 [ɪɴSPIRE].

[22] CMS collaboration, *Precision luminosity measurement in proton-proton collisions at $\sqrt{s} = 13$ TeV in 2015 and 2016 at CMS*, *Eur. Phys. J. C* **81** (2021) 800 [arXiv:2104.01927] [ɪɴSPIRE].

[23] M. Cacciari, G.P. Salam and G. Soyez, *The anti-$k_t$ jet clustering algorithm*, *JHEP* **04** (2008) 063 [arXiv:0802.1189] [InSPIRE].

[24] M. Cacciari, G.P. Salam and G. Soyez, *FastJet user manual*, *Eur. Phys. J. C* **72** (2012) 1896 [arXiv:1111.6097] [InSPIRE].

[25] D.J. Lange, *The EvtGen particle decay simulation package*, *Nucl. Instrum. Meth. A* **462** (2001) 152 [InSPIRE].

[26] GEANT4 collaboration, *GEANT4 — a simulation toolkit*, *Nucl. Instrum. Meth. A* **506** (2003) 250 [InSPIRE].

[27] PARTICLE DATA GROUP collaboration, *Review of particle physics*, *Phys. Rev. D* **98** (2018) 030001 [InSPIRE].

[28] CMS collaboration, *Measurement of tracking efficiency*, Tech. Rep. CMS-PAS-TRK-10-002, CERN, Geneva, Switzerland (2010).

[29] CMS collaboration, *Event generator tunes obtained from underlying event and multiparton scattering measurements*, *Eur. Phys. J. C* **76** (2016) 155 [arXiv:1512.00815] [InSPIRE].

[30] CMS collaboration, *Studies of beauty suppression via nonprompt $D^0$ mesons in Pb-Pb collisions at $Q^2 = 4\,GeV^2$*, *Phys. Rev. Lett.* **123** (2019) 022001 [arXiv:1810.11102] [InSPIRE].

[31] CMS collaboration, *Tracking POG results for pion efficiency with the $D^*$ meson using data from* 2016 *and* 2017, Tech. Rep. CMS-DP-2018-050, CERN, Geneva, Switzerland (2018).

[32] M.J. Oreglia, *A study of the reactions $\psi' \to \gamma\gamma\psi$*, Ph.D. thesis, SLAC report SLAC-R-236, Stanford University, Stanford, CA, U.S.A. (1980).

[33] J.E. Gaiser, *Charmonium spectroscopy from radiative decays of the $J/\psi$ and $\psi'$*, Ph.D. thesis, SLAC report SLAC-R-255, Stanford University, Stanford, CA, U.S.A. (1982).

[34] CMS collaboration, *CMS luminosity measurements for the* 2016 *data taking period*, Tech. Rep. CMS-PAS-LUM-17-001, CERN, Geneva, Switzerland (2017).

[35] M. Lisovyi, A. Verbytskyi and O. Zenaiev, *Combined analysis of charm-quark fragmentation-fraction measurements*, *Eur. Phys. J. C* **76** (2016) 397 [arXiv:1509.01061] [InSPIRE].

[36] ALICE collaboration, *Charm-quark fragmentation fractions and production cross section at midrapidity in pp collisions at the LHC*, arXiv:2105.06335 [InSPIRE].

[37] ALICE collaboration, *$\Lambda_c^+$ production in pp collisions at $\sqrt{s} = 7\,TeV$ and in p-Pb collisions at $\sqrt{s_{NN}} = 5.02\,TeV$*, *JHEP* **04** (2018) 108 [arXiv:1712.09581] [InSPIRE].

[38] ALICE collaboration, *$\Lambda_c^+$ production and baryon-to-meson ratios in pp and p-Pb collisions at $\sqrt{s_{NN}} = 5.02\,TeV$ at the LHC*, *Phys. Rev. Lett.* **127** (2021) 202301 [arXiv:2011.06078] [InSPIRE].

[39] ALICE collaboration, *$\Lambda_e^+$ production in pp and in p-Pb collisions at $\sqrt{s_{NN}} = 5.02\,TeV$*, *Phys. Rev. C* **104** (2021) 054905 [arXiv:2011.06079] [InSPIRE].

[40] CMS collaboration, *Production of $\Lambda_c^+$ baryons in proton-proton and lead-lead collisions at $\sqrt{s_{NN}} = 5.02\,TeV$*, *Phys. Lett. B* **803** (2020) 135328 [arXiv:1906.03322] [InSPIRE].

[41] CMS collaboration, *Study of the underlying event at forward rapidity in pp collisions at $\sqrt{s} = 0.9$, 2.76, *and* 7\,TeV*, *JHEP* **04** (2013) 072 [arXiv:1302.2394] [InSPIRE].

[42] R. Field, *Early LHC underlying event data — findings and surprises*, in 21<sup>st</sup> *hadron collider physics symposium*, (2010) [`arXiv:1010.3558`] [ɪɴSPIRE].

[43] ATLAS collaboration, *Summary of ATLAS PYTHIA 8 tunes*, Tech. Rep. ATL-PHYS-PUB-2012-003, CERN, Geneva, Switzerland (2012).

[44] R. Corke and T. Sjöstrand, *Interleaved parton showers and tuning prospects*, *JHEP* **03** (2011) 032 [`arXiv:1011.1759`] [ɪɴSPIRE].

[45] P. Skands, S. Carrazza and J. Rojo, *Tuning PYTHIA 8.1: the Monash 2013 tune*, *Eur. Phys. J. C* **74** (2014) 3024 [`arXiv:1404.5630`] [ɪɴSPIRE].

[46] CMS collaboration, *Extraction and validation of a new set of CMS PYTHIA8 tunes from underlying-event measurements*, *Eur. Phys. J. C* **80** (2020) 4 [`arXiv:1903.12179`] [ɪɴSPIRE].

## The CMS collaboration

### Yerevan Physics Institute, Yerevan, Armenia

A. Tumasyan

### Institut für Hochenergiephysik, Wien, Austria

W. Adam, F. Ambrogi, T. Bergauer, M. Dragicevic, J. Erö, A. Escalante Del Valle, R. Frühwirth[1], M. Jeitler[1], N. Krammer, L. Lechner, D. Liko, T. Madlener, I. Mikulec, F.M. Pitters, N. Rad, J. Schieck[1], R. Schöfbeck, M. Spanring, S. Templ, W. Waltenberger, C.-E. Wulz[1], M. Zarucki

### Institute for Nuclear Problems, Minsk, Belarus

V. Chekhovsky, A. Litomin, V. Makarenko, J. Suarez Gonzalez

### Universiteit Antwerpen, Antwerpen, Belgium

M.R. Darwish[2], E.A. De Wolf, D. Di Croce, X. Janssen, T. Kello[3], A. Lelek, M. Pieters, H. Rejeb Sfar, H. Van Haevermaet, P. Van Mechelen, S. Van Putte, N. Van Remortel

### Vrije Universiteit Brussel, Brussel, Belgium

F. Blekman, E.S. Bols, S.S. Chhibra, J. D'Hondt, J. De Clercq, D. Lontkovskyi, S. Lowette, I. Marchesini, S. Moortgat, A. Morton, Q. Python, S. Tavernier, W. Van Doninck, P. Van Mulders

### Université Libre de Bruxelles, Bruxelles, Belgium

D. Beghin, B. Bilin, B. Clerbaux, G. De Lentdecker, H. Delannoy, B. Dorney, L. Favart, A. Grebenyuk, A.K. Kalsi, I. Makarenko, L. Moureaux, L. Pétré, A. Popov, N. Postiau, E. Starling, L. Thomas, C. Vander Velde, P. Vanlaer, D. Vannerom, L. Wezenbeek

### Ghent University, Ghent, Belgium

T. Cornelis, D. Dobur, M. Gruchala, I. Khvastunov[4], M. Niedziela, C. Roskas, K. Skovpen, M. Tytgat, W. Verbeke, B. Vermassen, M. Vit

### Université Catholique de Louvain, Louvain-la-Neuve, Belgium

G. Bruno, F. Bury, C. Caputo, P. David, C. Delaere, M. Delcourt, I.S. Donertas, A. Giammanco, V. Lemaitre, K. Mondal, J. Prisciandaro, A. Taliercio, M. Teklishyn, P. Vischia, S. Wuyckens, J. Zobec

### Centro Brasileiro de Pesquisas Fisicas, Rio de Janeiro, Brazil

G.A. Alves, G. Correia Silva, C. Hensel, A. Moraes

### Universidade do Estado do Rio de Janeiro, Rio de Janeiro, Brazil

W.L. Aldá Júnior, E. Belchior Batista Das Chagas, H. BRANDAO MALBOUISSON, W. Carvalho, J. Chinellato[5], E. Coelho, E.M. Da Costa, G.G. Da Silveira[6], D. De Jesus Damiao, S. Fonseca De Souza, J. Martins[7], D. Matos Figueiredo, M. Medina Jaime[8], M. Melo De Almeida, C. Mora Herrera, L. Mundim, H. Nogima, P. Rebello Teles, L.J. Sanchez Rosas, A. Santoro, S.M. Silva Do Amaral, A. Sznajder, M. Thiel, E.J. Tonelli Manganote[5], F. Torres Da Silva De Araujo, A. Vilela Pereira

**Universidade Estadual Paulista [a], Universidade Federal do ABC [b], São Paulo, Brazil**

C.A. Bernardes[a], L. Calligaris[a], T.R. Fernandez Perez Tomei[a], E.M. Gregores[b], D.S. Lemos[a], P.G. Mercadante[b], S.F. Novaes[a], Sandra S. Padula[a]

**Institute for Nuclear Research and Nuclear Energy, Bulgarian Academy of Sciences, Sofia, Bulgaria**

A. Aleksandrov, G. Antchev, I. Atanasov, R. Hadjiiska, P. Iaydjiev, M. Misheva, M. Rodozov, M. Shopova, G. Sultanov

**University of Sofia, Sofia, Bulgaria**

M. Bonchev, A. Dimitrov, T. Ivanov, L. Litov, B. Pavlov, P. Petkov, A. Petrov

**Beihang University, Beijing, China**

W. Fang[3], Q. Guo, H. Wang, L. Yuan

**Department of Physics, Tsinghua University, Beijing, China**

M. Ahmad, Z. Hu, Y. Wang

**Institute of High Energy Physics, Beijing, China**

E. Chapon, G.M. Chen[9], H.S. Chen[9], M. Chen, D. Leggat, H. Liao, Z. Liu, R. Sharma, A. Spiezia, J. Tao, J. Thomas-Wilsker, J. Wang, H. Zhang, S. Zhang[9], J. Zhao

**State Key Laboratory of Nuclear Physics and Technology, Peking University, Beijing, China**

A. Agapitos, Y. Ban, C. Chen, A. Levin, Q. Li, M. Lu, X. Lyu, Y. Mao, S.J. Qian, D. Wang, Q. Wang, J. Xiao

**Sun Yat-Sen University, Guangzhou, China**

Z. You

**Institute of Modern Physics and Key Laboratory of Nuclear Physics and Ion-beam Application (MOE) — Fudan University, Shanghai, China**

X. Gao[3]

**Zhejiang University, Hangzhou, China**

M. Xiao

**Universidad de Los Andes, Bogota, Colombia**

C. Avila, A. Cabrera, C. Florez, J. Fraga, A. Sarkar, M.A. Segura Delgado

**Universidad de Antioquia, Medellin, Colombia**

J. Jaramillo, J. Mejia Guisao, F. Ramirez, J.D. Ruiz Alvarez, C.A. Salazar González, N. Vanegas Arbelaez

**University of Split, Faculty of Electrical Engineering, Mechanical Engineering and Naval Architecture, Split, Croatia**

D. Giljanovic, N. Godinovic, D. Lelas, I. Puljak, T. Sculac

**University of Split, Faculty of Science, Split, Croatia**
Z. Antunovic, M. Kovac

**Institute Rudjer Boskovic, Zagreb, Croatia**
V. Brigljevic, D. Ferencek, D. Majumder, B. Mesic, M. Roguljic, A. Starodumov[10], T. Susa

**University of Cyprus, Nicosia, Cyprus**
M.W. Ather, A. Attikis, E. Erodotou, A. Ioannou, G. Kole, M. Kolosova, S. Konstantinou,
G. Mavromanolakis, J. Mousa, C. Nicolaou, F. Ptochos, P.A. Razis, H. Rykaczewski,
H. Saka, D. Tsiakkouri

**Charles University, Prague, Czech Republic**
M. Finger[11], M. Finger Jr.[11], A. Kveton, J. Tomsa

**Escuela Politecnica Nacional, Quito, Ecuador**
E. Ayala

**Universidad San Francisco de Quito, Quito, Ecuador**
E. Carrera Jarrin

**Academy of Scientific Research and Technology of the Arab Republic of Egypt, Egyptian Network of High Energy Physics, Cairo, Egypt**
A.A. Abdelalim[12,13], S. Abu Zeid[14], S. Khalil[13]

**Center for High Energy Physics (CHEP-FU), Fayoum University, El-Fayoum, Egypt**
A. Lotfy, M.A. Mahmoud

**National Institute of Chemical Physics and Biophysics, Tallinn, Estonia**
S. Bhowmik, A. Carvalho Antunes De Oliveira, R.K. Dewanjee, K. Ehataht, M. Kadastik,
M. Raidal, C. Veelken

**Department of Physics, University of Helsinki, Helsinki, Finland**
P. Eerola, L. Forthomme, H. Kirschenmann, K. Osterberg, M. Voutilainen

**Helsinki Institute of Physics, Helsinki, Finland**
E. Brücken, F. Garcia, J. Havukainen, V. Karimäki, M.S. Kim, R. Kinnunen, T. Lampén,
K. Lassila-Perini, S. Laurila, S. Lehti, T. Lindén, H. Siikonen, E. Tuominen, J. Tuominiemi

**Lappeenranta University of Technology, Lappeenranta, Finland**
P. Luukka, T. Tuuva

**IRFU, CEA, Université Paris-Saclay, Gif-sur-Yvette, France**
C. Amendola, M. Besancon, F. Couderc, M. Dejardin, D. Denegri, J.L. Faure, F. Ferri,
S. Ganjour, A. Givernaud, P. Gras, G. Hamel de Monchenault, P. Jarry, B. Lenzi, E. Locci,
J. Malcles, J. Rander, A. Rosowsky, M.Ö. Sahin, A. Savoy-Navarro[15], M. Titov, G.B. Yu

**Laboratoire Leprince-Ringuet, CNRS/IN2P3, Ecole Polytechnique, Institut Polytechnique de Paris, Palaiseau, France**
S. Ahuja, F. Beaudette, M. Bonanomi, A. Buchot Perraguin, P. Busson, C. Charlot,
O. Davignon, B. Diab, G. Falmagne, R. Granier de Cassagnac, A. Hakimi, I. Kucher,

A. Lobanov, C. Martin Perez, M. Nguyen, C. Ochando, P. Paganini, J. Rembser, R. Salerno, J.B. Sauvan, Y. Sirois, A. Zabi, A. Zghiche

**Université de Strasbourg, CNRS, IPHC UMR 7178, Strasbourg, France**

J.-L. Agram[16], J. Andrea, D. Bloch, G. Bourgatte, J.-M. Brom, E.C. Chabert, C. Collard, J.-C. Fontaine[16], D. Gelé, U. Goerlach, C. Grimault, A.-C. Le Bihan, P. Van Hove

**Institut de Physique des 2 Infinis de Lyon (IP2I ), Villeurbanne, France**

E. Asilar, S. Beauceron, C. Bernet, G. Boudoul, C. Camen, A. Carle, N. Chanon, D. Contardo, P. Depasse, H. El Mamouni, J. Fay, S. Gascon, M. Gouzevitch, B. Ille, Sa. Jain, I.B. Laktineh, H. Lattaud, A. Lesauvage, M. Lethuillier, L. Mirabito, L. Torterotot, G. Touquet, M. Vander Donckt, S. Viret

**Georgian Technical University, Tbilisi, Georgia**

A. Khvedelidze[11], Z. Tsamalaidze[11]

**RWTH Aachen University, I. Physikalisches Institut, Aachen, Germany**

L. Feld, K. Klein, M. Lipinski, D. Meuser, A. Pauls, M. Preuten, M.P. Rauch, J. Schulz, M. Teroerde

**RWTH Aachen University, III. Physikalisches Institut A, Aachen, Germany**

D. Eliseev, M. Erdmann, P. Fackeldey, B. Fischer, S. Ghosh, T. Hebbeker, K. Hoepfner, H. Keller, L. Mastrolorenzo, M. Merschmeyer, A. Meyer, P. Millet, G. Mocellin, S. Mondal, S. Mukherjee, D. Noll, A. Novak, T. Pook, A. Pozdnyakov, T. Quast, M. Radziej, Y. Rath, H. Reithler, J. Roemer, A. Schmidt, S.C. Schuler, A. Sharma, S. Wiedenbeck, S. Zaleski

**RWTH Aachen University, III. Physikalisches Institut B, Aachen, Germany**

C. Dziwok, G. Flügge, W. Haj Ahmad[17], O. Hlushchenko, T. Kress, A. Nowack, C. Pistone, O. Pooth, D. Roy, H. Sert, A. Stahl[18], T. Ziemons

**Deutsches Elektronen-Synchrotron, Hamburg, Germany**

H. Aarup Petersen, M. Aldaya Martin, P. Asmuss, I. Babounikau, S. Baxter, O. Behnke, A. Bermúdez Martínez, A.A. Bin Anuar, K. Borras[19], V. Botta, D. Brunner, A. Campbell, A. Cardini, P. Connor, S. Consuegra Rodríguez, V. Danilov, A. De Wit, M.M. Defranchis, L. Didukh, D. Domínguez Damiani, G. Eckerlin, D. Eckstein, T. Eichhorn, A. Elwood, L.I. Estevez Banos, E. Gallo[20], A. Geiser, A. Giraldi, A. Grohsjean, M. Guthoff, A. Harb, A. Jafari[21], N.Z. Jomhari, H. Jung, A. Kasem[19], M. Kasemann, H. Kaveh, C. Kleinwort, J. Knolle, D. Krücker, W. Lange, T. Lenz, J. Lidrych, K. Lipka, W. Lohmann[22], R. Mankel, I.-A. Melzer-Pellmann, J. Metwally, A.B. Meyer, M. Meyer, M. Missiroli, J. Mnich, A. Mussgiller, V. Myronenko, Y. Otarid, D. Pérez Adán, S.K. Pflitsch, D. Pitzl, A. Raspereza, A. Saggio, A. Saibel, M. Savitskyi, V. Scheurer, P. Schütze, C. Schwanenberger, R. Shevchenko, A. Singh, R.E. Sosa Ricardo, H. Tholen, N. Tonon, O. Turkot, A. Vagnerini, M. Van De Klundert, R. Walsh, D. Walter, Y. Wen, K. Wichmann, C. Wissing, S. Wuchterl, Y. Yang, O. Zenaiev, R. Zlebcik

**University of Hamburg, Hamburg, Germany**

R. Aggleton, S. Bein, L. Benato, A. Benecke, K. De Leo, T. Dreyer, A. Ebrahimi, M. Eich, F. Feindt, A. Fröhlich, C. Garbers, E. Garutti, P. Gunnellini, J. Haller, A. Hinzmann,

A. Karavdina, G. Kasieczka, R. Klanner, R. Kogler, V. Kutzner, J. Lange, T. Lange, A. Malara, J. Multhaup, C.E.N. Niemeyer, A. Nigamova, K.J. Pena Rodriguez, O. Rieger, P. Schleper, S. Schumann, J. Schwandt, D. Schwarz, J. Sonneveld, H. Stadie, G. Steinbrück, B. Vormwald, I. Zoi

**Karlsruher Institut fuer Technologie, Karlsruhe, Germany**

M. Baselga, S. Baur, J. Bechtel, T. Berger, E. Butz, R. Caspart, T. Chwalek, W. De Boer, A. Dierlamm, A. Droll, K. El Morabit, N. Faltermann, K. Flöh, M. Giffels, A. Gottmann, F. Hartmann[18], C. Heidecker, U. Husemann, M.A. Iqbal, I. Katkov[23], P. Keicher, R. Koppenhöfer, S. Maier, M. Metzler, S. Mitra, M.U. Mozer, D. Müller, Th. Müller, M. Musich, G. Quast, K. Rabbertz, J. Rauser, D. Savoiu, D. Schäfer, M. Schnepf, M. Schröder, D. Seith, I. Shvetsov, H.J. Simonis, R. Ulrich, M. Wassmer, M. Weber, C. Wöhrmann, R. Wolf, S. Wozniewski

**Institute of Nuclear and Particle Physics (INPP), NCSR Demokritos, Aghia Paraskevi, Greece**

G. Anagnostou, P. Asenov, G. Daskalakis, T. Geralis, A. Kyriakis, D. Loukas, G. Paspalaki, A. Stakia

**National and Kapodistrian University of Athens, Athens, Greece**

M. Diamantopoulou, D. Karasavvas, G. Karathanasis, P. Kontaxakis, C.K. Koraka, A. Manousakis-Katsikakis, A. Panagiotou, I. Papavergou, N. Saoulidou, K. Theofilatos, K. Vellidis, E. Vourliotis

**National Technical University of Athens, Athens, Greece**

G. Bakas, K. Kousouris, I. Papakrivopoulos, G. Tsipolitis, A. Zacharopoulou

**University of Ioánnina, Ioánnina, Greece**

I. Evangelou, C. Foudas, P. Gianneios, P. Katsoulis, P. Kokkas, S. Mallios, K. Manitara, N. Manthos, I. Papadopoulos, J. Strologas

**MTA-ELTE Lendület CMS Particle and Nuclear Physics Group, Eötvös Loránd University, Budapest, Hungary**

M. Bartók[24], R. Chudasama, M. Csanad, M.M.A. Gadallah[25], S. Lökös[26], P. Major, K. Mandal, A. Mehta, G. Pasztor, O. Surányi, G.I. Veres

**Wigner Research Centre for Physics, Budapest, Hungary**

G. Bencze, C. Hajdu, D. Horvath[27], F. Sikler, V. Veszpremi, G. Vesztergombi[†]

**Institute of Nuclear Research ATOMKI, Debrecen, Hungary**

S. Czellar, J. Karancsi[24], J. Molnar, Z. Szillasi, D. Teyssier

**Institute of Physics, University of Debrecen, Debrecen, Hungary**

P. Raics, Z.L. Trocsanyi, B. Ujvari

**Karoly Robert Campus, MATE Institute of Technology**

T. Csorgo, F. Nemes, T. Novak

**Indian Institute of Science (IISc), Bangalore, India**

S. Choudhury, J.R. Komaragiri, D. Kumar, L. Panwar, P.C. Tiwari

**National Institute of Science Education and Research, HBNI, Bhubaneswar, India**

S. Bahinipati[28], D. Dash, C. Kar, P. Mal, T. Mishra, V.K. Muraleedharan Nair Bindhu, A. Nayak[29], D.K. Sahoo[28], N. Sur, S.K. Swain

**Panjab University, Chandigarh, India**

S. Bansal, S.B. Beri, V. Bhatnagar, S. Chauhan, N. Dhingra[30], R. Gupta, A. Kaur, S. Kaur, P. Kumari, M. Lohan, M. Meena, K. Sandeep, S. Sharma, J.B. Singh, A.K. Virdi

**University of Delhi, Delhi, India**

A. Ahmed, A. Bhardwaj, B.C. Choudhary, R.B. Garg, M. Gola, S. Keshri, A. Kumar, M. Naimuddin, P. Priyanka, K. Ranjan, A. Shah

**Saha Institute of Nuclear Physics, HBNI, Kolkata, India**

M. Bharti[31], R. Bhattacharya, S. Bhattacharya, D. Bhowmik, S. Dutta, S. Ghosh, B. Gomber[32], M. Maity[33], S. Nandan, P. Palit, A. Purohit, P.K. Rout, G. Saha, S. Sarkar, M. Sharan, B. Singh[31], S. Thakur[31]

**Indian Institute of Technology Madras, Madras, India**

P.K. Behera, S.C. Behera, P. Kalbhor, A. Muhammad, R. Pradhan, P.R. Pujahari, A. Sharma, A.K. Sikdar

**Bhabha Atomic Research Centre, Mumbai, India**

D. Dutta, V. Jha, V. Kumar, D.K. Mishra, K. Naskar[34], P.K. Netrakanti, L.M. Pant, P. Shukla

**Tata Institute of Fundamental Research-A, Mumbai, India**

T. Aziz, M.A. Bhat, S. Dugad, R. Kumar Verma, U. Sarkar

**Tata Institute of Fundamental Research-B, Mumbai, India**

S. Banerjee, S. Bhattacharya, S. Chatterjee, P. Das, M. Guchait, S. Karmakar, S. Kumar, G. Majumder, K. Mazumdar, S. Mukherjee, D. Roy, N. Sahoo

**Indian Institute of Science Education and Research (IISER), Pune, India**

S. Dube, B. Kansal, A. Kapoor, K. Kothekar, S. Pandey, A. Rane, A. Rastogi, S. Sharma

**Department of Physics, Isfahan University of Technology, Isfahan, Iran**

H. Bakhshiansohi[35]

**Institute for Research in Fundamental Sciences (IPM), Tehran, Iran**

S. Chenarani[36], S.M. Etesami, M. Khakzad, M. Mohammadi Najafabadi

**University College Dublin, Dublin, Ireland**

M. Felcini, M. Grunewald

**INFN Sezione di Bari $^a$, Università di Bari $^b$, Politecnico di Bari $^c$, Bari, Italy**

M. Abbrescia$^{a,b}$, R. Aly$^{a,b,37}$, C. Aruta$^{a,b}$, A. Colaleo$^a$, D. Creanza$^{a,c}$, N. De Filippis$^{a,c}$, M. De Palma$^{a,b}$, A. Di Florio$^{a,b}$, A. Di Pilato$^{a,b}$, W. Elmetenawee$^{a,b}$, L. Fiore$^a$, A. Gelmi$^{a,b}$, M. Gul$^a$, G. Iaselli$^{a,c}$, M. Ince$^{a,b}$, S. Lezki$^{a,b}$, G. Maggi$^{a,c}$, M. Maggi$^a$, I. Margjeka$^{a,b}$, J.A. Merlin$^a$, S. My$^{a,b}$, S. Nuzzo$^{a,b}$, A. Pompili$^{a,b}$, G. Pugliese$^{a,c}$, A. Ranieri$^a$, G. Selvaggi$^{a,b}$, L. Silvestris$^a$, F.M. Simone$^{a,b}$, R. Venditti$^a$, P. Verwilligen$^a$

**INFN Sezione di Bologna $^a$, Università di Bologna $^b$, Bologna, Italy**

G. Abbiendi$^a$, C. Battilana$^{a,b}$, D. Bonacorsi$^{a,b}$, L. Borgonovi$^{a,b}$, S. Braibant-Giacomelli$^{a,b}$, R. Campanini$^{a,b}$, P. Capiluppi$^{a,b}$, A. Castro$^{a,b}$, F.R. Cavallo$^a$, C. Ciocca$^a$, M. Cuffiani$^{a,b}$, G.M. Dallavalle$^a$, T. Diotalevi$^{a,b}$, F. Fabbri$^a$, A. Fanfani$^{a,b}$, E. Fontanesi$^{a,b}$, P. Giacomelli$^a$, L. Giommi$^{a,b}$, C. Grandi$^a$, L. Guiducci$^{a,b}$, F. Iemmi$^{a,b}$, S. Lo Meo$^{a,38}$, S. Marcellini$^a$, G. Masetti$^a$, F.L. Navarria$^{a,b}$, A. Perrotta$^a$, F. Primavera$^{a,b}$, T. Rovelli$^{a,b}$, G.P. Siroli$^{a,b}$, N. Tosi$^a$

**INFN Sezione di Catania $^a$, Università di Catania $^b$, Catania, Italy**

S. Albergo$^{a,b,39}$, S. Costa$^{a,b,39}$, A. Di Mattia$^a$, R. Potenza$^{a,b}$, A. Tricomi$^{a,b,39}$, C. Tuve$^{a,b}$

**INFN Sezione di Firenze $^a$, Università di Firenze $^b$, Firenze, Italy**

G. Barbagli$^a$, A. Cassese$^a$, R. Ceccarelli$^{a,b}$, V. Ciulli$^{a,b}$, C. Civinini$^a$, R. D'Alessandro$^{a,b}$, F. Fiori$^a$, E. Focardi$^{a,b}$, G. Latino$^{a,b}$, P. Lenzi$^{a,b}$, M. Lizzo$^{a,b}$, M. Meschini$^a$, S. Paoletti$^a$, R. Seidita$^{a,b}$, G. Sguazzoni$^a$, L. Viliani$^a$

**INFN Laboratori Nazionali di Frascati, Frascati, Italy**

L. Benussi, S. Bianco, D. Piccolo

**INFN Sezione di Genova $^a$, Università di Genova $^b$, Genova, Italy**

M. Bozzo$^{a,b}$, F. Ferro$^a$, R. Mulargia$^{a,b}$, E. Robutti$^a$, S. Tosi$^{a,b}$

**INFN Sezione di Milano-Bicocca $^a$, Università di Milano-Bicocca $^b$, Milano, Italy**

A. Benaglia$^a$, A. Beschi$^{a,b}$, F. Brivio$^{a,b}$, F. Cetorelli$^{a,b}$, V. Ciriolo$^{a,b,18}$, F. De Guio$^{a,b}$, M.E. Dinardo$^{a,b}$, P. Dini$^a$, S. Gennai$^a$, A. Ghezzi$^{a,b}$, P. Govoni$^{a,b}$, L. Guzzi$^{a,b}$, M. Malberti$^a$, S. Malvezzi$^a$, D. Menasce$^a$, F. Monti$^{a,b}$, L. Moroni$^a$, M. Paganoni$^{a,b}$, D. Pedrini$^a$, S. Ragazzi$^{a,b}$, T. Tabarelli de Fatis$^{a,b}$, D. Valsecchi$^{a,b,18}$, D. Zuolo$^{a,b}$

**INFN Sezione di Napoli $^a$, Università di Napoli 'Federico II' $^b$, Napoli, Italy, Università della Basilicata $^c$, Potenza, Italy, Università G. Marconi $^d$, Roma, Italy**

S. Buontempo$^a$, N. Cavallo$^{a,c}$, A. De Iorio$^{a,b}$, F. Fabozzi$^{a,c}$, F. Fienga$^a$, A.O.M. Iorio$^{a,b}$, L. Layer$^{a,b}$, L. Lista$^{a,b}$, S. Meola$^{a,d,18}$, P. Paolucci$^{a,18}$, B. Rossi$^a$, C. Sciacca$^{a,b}$, E. Voevodina$^{a,b}$

**INFN Sezione di Padova $^a$, Università di Padova $^b$, Padova, Italy, Università di Trento $^c$, Trento, Italy**

P. Azzi$^a$, N. Bacchetta$^a$, D. Bisello$^{a,b}$, A. Boletti$^{a,b}$, A. Bragagnolo$^{a,b}$, R. Carlin$^{a,b}$, P. Checchia$^a$, P. De Castro Manzano$^a$, T. Dorigo$^a$, F. Gasparini$^{a,b}$, U. Gasparini$^{a,b}$,

S.Y. Hoh$^{a,b}$, M. Margoni$^{a,b}$, A.T. Meneguzzo$^{a,b}$, M. Presilla$^{b}$, P. Ronchese$^{a,b}$, R. Rossin$^{a,b}$, F. Simonetto$^{a,b}$, G. Strong, A. Tiko$^{a}$, M. Tosi$^{a,b}$, H. YARAR$^{a,b}$, M. Zanetti$^{a,b}$, P. Zotto$^{a,b}$, A. Zucchetta$^{a,b}$

**INFN Sezione di Pavia $^a$, Università di Pavia $^b$, Pavia, Italy**

A. Braghieri$^{a}$, S. Calzaferri$^{a,b}$, D. Fiorina$^{a,b}$, P. Montagna$^{a,b}$, S.P. Ratti$^{a,b}$, V. Re$^{a}$, M. Ressegotti$^{a,b}$, C. Riccardi$^{a,b}$, P. Salvini$^{a}$, I. Vai$^{a}$, P. Vitulo$^{a,b}$

**INFN Sezione di Perugia $^a$, Università di Perugia $^b$, Perugia, Italy**

M. Biasini$^{a,b}$, G.M. Bilei$^{a}$, D. Ciangottini$^{a,b}$, L. Fanò$^{a,b}$, P. Lariccia$^{a,b}$, G. Mantovani$^{a,b}$, V. Mariani$^{a,b}$, M. Menichelli$^{a}$, F. Moscatelli$^{a}$, A. Rossi$^{a,b}$, A. Santocchia$^{a,b}$, D. Spiga$^{a}$, T. Tedeschi$^{a,b}$

**INFN Sezione di Pisa $^a$, Università di Pisa $^b$, Scuola Normale Superiore di Pisa $^c$, Pisa Italy, Università di Siena $^d$, Siena, Italy**

K. Androsov$^{a}$, P. Azzurri$^{a}$, G. Bagliesi$^{a}$, V. Bertacchi$^{a,c}$, L. Bianchini$^{a}$, T. Boccali$^{a}$, R. Castaldi$^{a}$, M.A. Ciocci$^{a,b}$, R. Dell'Orso$^{a}$, M.R. Di Domenico$^{a,d}$, S. Donato$^{a}$, L. Giannini$^{a,c}$, A. Giassi$^{a}$, M.T. Grippo$^{a}$, F. Ligabue$^{a,c}$, E. Manca$^{a,c}$, G. Mandorli$^{a,c}$, A. Messineo$^{a,b}$, F. Palla$^{a}$, G. Ramirez-Sanchez$^{a,c}$, A. Rizzi$^{a,b}$, G. Rolandi$^{a,c}$, S. Roy Chowdhury$^{a,c}$, A. Scribano$^{a}$, N. Shafiei$^{a,b}$, P. Spagnolo$^{a}$, R. Tenchini$^{a}$, G. Tonelli$^{a,b}$, N. Turini$^{a,d}$, A. Venturi$^{a}$, P.G. Verdini$^{a}$

**INFN Sezione di Roma $^a$, Sapienza Università di Roma $^b$, Rome, Italy**

F. Cavallari$^{a}$, M. Cipriani$^{a,b}$, D. Del Re$^{a,b}$, E. Di Marco$^{a}$, M. Diemoz$^{a}$, E. Longo$^{a,b}$, P. Meridiani$^{a}$, G. Organtini$^{a,b}$, F. Pandolfi$^{a}$, R. Paramatti$^{a,b}$, C. Quaranta$^{a,b}$, S. Rahatlou$^{a,b}$, C. Rovelli$^{a}$, F. Santanastasio$^{a,b}$, L. Soffi$^{a,b}$, R. Tramontano$^{a,b}$

**INFN Sezione di Torino $^a$, Università di Torino $^b$, Torino, Italy, Università del Piemonte Orientale $^c$, Novara, Italy**

N. Amapane$^{a,b}$, R. Arcidiacono$^{a,c}$, S. Argiro$^{a,b}$, M. Arneodo$^{a,c}$, N. Bartosik$^{a}$, R. Bellan$^{a,b}$, A. Bellora$^{a,b}$, C. Biino$^{a}$, A. Cappati$^{a,b}$, N. Cartiglia$^{a}$, S. Cometti$^{a}$, M. Costa$^{a,b}$, R. Covarelli$^{a,b}$, N. Demaria$^{a}$, B. Kiani$^{a,b}$, F. Legger$^{a}$, C. Mariotti$^{a}$, S. Maselli$^{a}$, E. Migliore$^{a,b}$, V. Monaco$^{a,b}$, E. Monteil$^{a,b}$, M. Monteno$^{a}$, M.M. Obertino$^{a,b}$, G. Ortona$^{a}$, L. Pacher$^{a,b}$, N. Pastrone$^{a}$, M. Pelliccioni$^{a}$, G.L. Pinna Angioni$^{a,b}$, M. Ruspa$^{a,c}$, R. Salvatico$^{a,b}$, F. Siviero$^{a,b}$, V. Sola$^{a}$, A. Solano$^{a,b}$, D. Soldi$^{a,b}$, A. Staiano$^{a}$, D. Trocino$^{a,b}$

**INFN Sezione di Trieste $^a$, Università di Trieste $^b$, Trieste, Italy**

S. Belforte$^{a}$, V. Candelise$^{a,b}$, M. Casarsa$^{a}$, F. Cossutti$^{a}$, A. Da Rold$^{a,b}$, G. Della Ricca$^{a,b}$, F. Vazzoler$^{a,b}$

**Kyungpook National University, Daegu, Korea**

S. Dogra, C. Huh, B. Kim, D.H. Kim, G.N. Kim, J. Lee, S.W. Lee, C.S. Moon, Y.D. Oh, S.I. Pak, B.C. Radburn-Smith, S. Sekmen, Y.C. Yang

**Chonnam National University, Institute for Universe and Elementary Particles, Kwangju, Korea**

H. Kim, D.H. Moon

**Hanyang University, Seoul, Korea**
B. Francois, T.J. Kim, J. Park

**Korea University, Seoul, Korea**
S. Cho, S. Choi, Y. Go, S. Ha, B. Hong, K. Lee, K.S. Lee, J. Lim, J. Park, S.K. Park, J. Yoo

**Kyung Hee University, Department of Physics, Seoul, Republic of Korea**
J. Goh, A. Gurtu

**Sejong University, Seoul, Korea**
H.S. Kim, Y. Kim

**Seoul National University, Seoul, Korea**
J. Almond, J.H. Bhyun, J. Choi, S. Jeon, J. Kim, J.S. Kim, S. Ko, H. Kwon, H. Lee, K. Lee, S. Lee, K. Nam, B.H. Oh, M. Oh, S.B. Oh, H. Seo, U.K. Yang, I. Yoon

**University of Seoul, Seoul, Korea**
D. Jeon, J.H. Kim, B. Ko, J.S.H. Lee, I.C. Park, Y. Roh, D. Song, I.J. Watson

**Yonsei University, Department of Physics, Seoul, Korea**
H.D. Yoo

**Sungkyunkwan University, Suwon, Korea**
Y. Choi, C. Hwang, Y. Jeong, H. Lee, Y. Lee, I. Yu

**College of Engineering and Technology, American University of the Middle East (AUM), Egaila, Kuwait**
Y. Maghrbi

**Riga Technical University, Riga, Latvia**
V. Veckalns[40]

**Vilnius University, Vilnius, Lithuania**
A. Juodagalvis, A. Rinkevicius, G. Tamulaitis

**National Centre for Particle Physics, Universiti Malaya, Kuala Lumpur, Malaysia**
W.A.T. Wan Abdullah, M.N. Yusli, Z. Zolkapli

**Universidad de Sonora (UNISON), Hermosillo, Mexico**
J.F. Benitez, A. Castaneda Hernandez, J.A. Murillo Quijada, L. Valencia Palomo

**Centro de Investigacion y de Estudios Avanzados del IPN, Mexico City, Mexico**
H. Castilla-Valdez, E. De La Cruz-Burelo, I. Heredia-De La Cruz[41], R. Lopez-Fernandez, A. Sanchez-Hernandez

**Universidad Iberoamericana, Mexico City, Mexico**
S. Carrillo Moreno, C. Oropeza Barrera, M. Ramirez-Garcia, F. Vazquez Valencia

**Benemerita Universidad Autonoma de Puebla, Puebla, Mexico**
J. Eysermans, I. Pedraza, H.A. Salazar Ibarguen, C. Uribe Estrada

**Universidad Autónoma de San Luis Potosí, San Luis Potosí, Mexico**

A. Morelos Pineda

**University of Montenegro, Podgorica, Montenegro**

J. Mijuskovic[4], N. Raicevic

**University of Auckland, Auckland, New Zealand**

D. Krofcheck

**University of Canterbury, Christchurch, New Zealand**

S. Bheesette, P.H. Butler

**National Centre for Physics, Quaid-I-Azam University, Islamabad, Pakistan**

A. Ahmad, M.I. Asghar, M.I.M. Awan, Q. Hassan, H.R. Hoorani, W.A. Khan, M.A. Shah, M. Shoaib, M. Waqas

**AGH University of Science and Technology Faculty of Computer Science, Electronics and Telecommunications, Krakow, Poland**

V. Avati, L. Grzanka, M. Malawski

**National Centre for Nuclear Research, Swierk, Poland**

H. Bialkowska, M. Bluj, B. Boimska, T. Frueboes, M. Górski, M. Kazana, M. Szleper, P. Traczyk, P. Zalewski

**Institute of Experimental Physics, Faculty of Physics, University of Warsaw, Warsaw, Poland**

K. Bunkowski, A. Byszuk[42], K. Doroba, A. Kalinowski, M. Konecki, J. Krolikowski, M. Olszewski, M. Walczak

**Laboratório de Instrumentação e Física Experimental de Partículas, Lisboa, Portugal**

M. Araujo, P. Bargassa, D. Bastos, P. Faccioli, M. Gallinaro, J. Hollar, N. Leonardo, T. Niknejad, J. Seixas, K. Shchelina, O. Toldaiev, J. Varela

**Joint Institute for Nuclear Research, Dubna, Russia**

S. Afanasiev, V. Alexakhin, P. Bunin, Y. Ershov, M. Gavrilenko, A. Golunov, I. Golutvin, N. Gorbounov, I. Gorbunov, A. Kamenev, V. Karjavine, A. Lanev, A. Malakhov, V. Matveev[43,44], P. Moisenz, V. Palichik, V. Perelygin, M. Savina, S. Shmatov, S. Shulha, V. Smirnov, O. Teryaev, A. Zarubin

**Petersburg Nuclear Physics Institute, Gatchina (St. Petersburg), Russia**

G. Gavrilov, V. Golovtcov, Y. Ivanov, V. Kim[45], E. Kuznetsova[46], V. Murzin, V. Oreshkin, I. Smirnov, D. Sosnov, V. Sulimov, L. Uvarov, S. Volkov, A. Vorobyev

**Institute for Nuclear Research, Moscow, Russia**

Yu. Andreev, A. Dermenev, S. Gninenko, N. Golubev, A. Karneyeu, M. Kirsanov, N. Krasnikov, A. Pashenkov, G. Pivovarov, D. Tlisov[†], A. Toropin

**Institute for Theoretical and Experimental Physics named by A.I. Alikhanov of NRC 'Kurchatov Institute', Moscow, Russia**

V. Epshteyn, V. Gavrilov, N. Lychkovskaya, A. Nikitenko[47], V. Popov, I. Pozdnyakov, G. Safronov, A. Spiridonov, A. Stepennov, M. Toms, E. Vlasov, A. Zhokin

**Moscow Institute of Physics and Technology, Moscow, Russia**

T. Aushev

**National Research Nuclear University 'Moscow Engineering Physics Institute' (MEPhI), Moscow, Russia**

R. Chistov[48], M. Danilov[48], A. Oskin, P. Parygin, S. Polikarpov[48]

**P.N. Lebedev Physical Institute, Moscow, Russia**

V. Andreev, M. Azarkin, I. Dremin, M. Kirakosyan, A. Terkulov

**Skobeltsyn Institute of Nuclear Physics, Lomonosov Moscow State University, Moscow, Russia**

A. Belyaev, E. Boos, M. Dubinin[49], L. Dudko, A. Ershov, A. Gribushin, V. Klyukhin, O. Kodolova, I. Lokhtin, S. Obraztsov, S. Petrushanko, V. Savrin, A. Snigirev

**Novosibirsk State University (NSU), Novosibirsk, Russia**

V. Blinov[50], T. Dimova[50], L. Kardapoltsev[50], I. Ovtin[50], Y. Skovpen[50]

**Institute for High Energy Physics of National Research Centre 'Kurchatov Institute', Protvino, Russia**

I. Azhgirey, I. Bayshev, V. Kachanov, A. Kalinin, D. Konstantinov, V. Petrov, R. Ryutin, A. Sobol, S. Troshin, N. Tyurin, A. Uzunian, A. Volkov

**National Research Tomsk Polytechnic University, Tomsk, Russia**

A. Babaev, A. Iuzhakov, V. Okhotnikov, L. Sukhikh

**Tomsk State University, Tomsk, Russia**

V. Borchsh, V. Ivanchenko, E. Tcherniaev

**University of Belgrade: Faculty of Physics and VINCA Institute of Nuclear Sciences, Belgrade, Serbia**

P. Adzic[51], P. Cirkovic, M. Dordevic, P. Milenovic, J. Milosevic

**Centro de Investigaciones Energéticas Medioambientales y Tecnológicas (CIEMAT), Madrid, Spain**

M. Aguilar-Benitez, J. Alcaraz Maestre, A. Álvarez Fernández, I. Bachiller, M. Barrio Luna, Cristina F. Bedoya, J.A. Brochero Cifuentes, C.A. Carrillo Montoya, M. Cepeda, M. Cerrada, N. Colino, B. De La Cruz, A. Delgado Peris, J.P. Fernández Ramos, J. Flix, M.C. Fouz, A. García Alonso, O. Gonzalez Lopez, S. Goy Lopez, J.M. Hernandez, M.I. Josa, J. León Holgado, D. Moran, Á. Navarro Tobar, A. Pérez-Calero Yzquierdo, J. Puerta Pelayo, I. Redondo, L. Romero, S. Sánchez Navas, M.S. Soares, A. Triossi, L. Urda Gómez, C. Willmott

**Universidad Autónoma de Madrid, Madrid, Spain**

C. Albajar, J.F. de Trocóniz, R. Reyes-Almanza

**Universidad de Oviedo, Instituto Universitario de Ciencias y Tecnologías Espaciales de Asturias (ICTEA), Oviedo, Spain**

B. Alvarez Gonzalez, J. Cuevas, C. Erice, J. Fernandez Menendez, S. Folgueras, I. Gonzalez Caballero, E. Palencia Cortezon, C. Ramón Álvarez, J. Ripoll Sau, V. Rodríguez Bouza, S. Sanchez Cruz, A. Trapote

**Instituto de Física de Cantabria (IFCA), CSIC-Universidad de Cantabria, Santander, Spain**

I.J. Cabrillo, A. Calderon, B. Chazin Quero, J. Duarte Campderros, M. Fernandez, P.J. Fernández Manteca, G. Gomez, C. Martinez Rivero, P. Martinez Ruiz del Arbol, F. Matorras, J. Piedra Gomez, C. Prieels, F. Ricci-Tam, T. Rodrigo, A. Ruiz-Jimeno, L. Russo[52], L. Scodellaro, I. Vila, J.M. Vizan Garcia

**University of Colombo, Colombo, Sri Lanka**

M.K. Jayananda, B. Kailasapathy[53], D.U.J. Sonnadara, D.D.C. Wickramarathna

**University of Ruhuna, Department of Physics, Matara, Sri Lanka**

W.G.D. Dharmaratna, K. Liyanage, N. Perera, N. Wickramage

**CERN, European Organization for Nuclear Research, Geneva, Switzerland**

T.K. Aarrestad, D. Abbaneo, B. Akgun, E. Auffray, G. Auzinger, J. Baechler, P. Baillon, A.H. Ball, D. Barney, J. Bendavid, N. Beni, M. Bianco, A. Bocci, P. Bortignon, E. Bossini, E. Brondolin, T. Camporesi, G. Cerminara, L. Cristella, D. d'Enterria, A. Dabrowski, N. Daci, V. Daponte, A. David, A. De Roeck, M. Deile, R. Di Maria, M. Dobson, M. Dünser, N. Dupont, A. Elliott-Peisert, N. Emriskova, F. Fallavollita[54], D. Fasanella, S. Fiorendi, G. Franzoni, J. Fulcher, W. Funk, S. Giani, D. Gigi, K. Gill, F. Glege, L. Gouskos, M. Guilbaud, D. Gulhan, M. Haranko, J. Hegeman, Y. Iiyama, V. Innocente, T. James, P. Janot, J. Kaspar, J. Kieseler, M. Komm, N. Kratochwil, C. Lange, P. Lecoq, K. Long, C. Lourenço, L. Malgeri, M. Mannelli, A. Massironi, F. Meijers, S. Mersi, E. Meschi, F. Moortgat, M. Mulders, J. Ngadiuba, J. Niedziela, S. Orfanelli, L. Orsini, F. Pantaleo[18], L. Pape, E. Perez, M. Peruzzi, A. Petrilli, G. Petrucciani, A. Pfeiffer, M. Pierini, D. Rabady, A. Racz, M. Rieger, M. Rovere, H. Sakulin, J. Salfeld-Nebgen, S. Scarfi, C. Schäfer, C. Schwick, M. Selvaggi, A. Sharma, P. Silva, W. Snoeys, P. Sphicas[55], J. Steggemann, S. Summers, V.R. Tavolaro, D. Treille, A. Tsirou, G.P. Van Onsem, A. Vartak, M. Verzetti, K.A. Wozniak, W.D. Zeuner

**Paul Scherrer Institut, Villigen, Switzerland**

L. Caminada[56], W. Erdmann, R. Horisberger, Q. Ingram, H.C. Kaestli, D. Kotlinski, U. Langenegger, T. Rohe

**ETH Zurich — Institute for Particle Physics and Astrophysics (IPA), Zurich, Switzerland**

M. Backhaus, P. Berger, A. Calandri, N. Chernyavskaya, G. Dissertori, M. Dittmar, M. Donegà, C. Dorfer, T. Gadek, T.A. Gómez Espinosa, C. Grab, D. Hits, W. Lustermann,

A.-M. Lyon, R.A. Manzoni, M.T. Meinhard, F. Micheli, F. Nessi-Tedaldi, F. Pauss, V. Perovic, G. Perrin, L. Perrozzi, S. Pigazzini, M.G. Ratti, M. Reichmann, C. Reissel, T. Reitenspiess, B. Ristic, D. Ruini, D.A. Sanz Becerra, M. Schönenberger, L. Shchutska, V. Stampf, M.L. Vesterbacka Olsson, R. Wallny, D.H. Zhu

**Universität Zürich, Zurich, Switzerland**

C. Amsler[57], C. Botta, D. Brzhechko, M.F. Canelli, A. De Cosa, R. Del Burgo, J.K. Heikkilä, M. Huwiler, A. Jofrehei, B. Kilminster, S. Leontsinis, A. Macchiolo, P. Meiring, V.M. Mikuni, U. Molinatti, I. Neutelings, G. Rauco, A. Reimers, P. Robmann, K. Schweiger, Y. Takahashi, S. Wertz

**National Central University, Chung-Li, Taiwan**

C. Adloff[58], C.M. Kuo, W. Lin, A. Roy, T. Sarkar[33], S.S. Yu

**National Taiwan University (NTU), Taipei, Taiwan**

L. Ceard, P. Chang, Y. Chao, K.F. Chen, P.H. Chen, W.-S. Hou, Y.y. Li, R.-S. Lu, E. Paganis, A. Psallidas, A. Steen, E. Yazgan

**Chulalongkorn University, Faculty of Science, Department of Physics, Bangkok, Thailand**

B. Asavapibhop, C. Asawatangtrakuldee, N. Srimanobhas

**Çukurova University, Physics Department, Science and Art Faculty, Adana, Turkey**

F. Boran, S. Damarseckin[59], Z.S. Demiroglu, F. Dolek, C. Dozen[60], I. Dumanoglu[61], E. Eskut, G. Gokbulut, Y. Guler, E. Gurpinar Guler[62], I. Hos[63], C. Isik, E.E. Kangal[64], O. Kara, A. Kayis Topaksu, U. Kiminsu, G. Onengut, K. Ozdemir[65], A. Polatoz, A.E. Simsek, B. Tali[66], U.G. Tok, S. Turkcapar, I.S. Zorbakir, C. Zorbilmez

**Middle East Technical University, Physics Department, Ankara, Turkey**

B. Isildak[67], G. Karapinar[68], K. Ocalan[69], M. Yalvac[70]

**Bogazici University, Istanbul, Turkey**

I.O. Atakisi, E. Gülmez, M. Kaya[71], O. Kaya[72], Ö. Özçelik, S. Tekten[73], E.A. Yetkin[74]

**Istanbul Technical University, Istanbul, Turkey**

A. Cakir, K. Cankocak[61], Y. Komurcu, S. Sen[75]

**Istanbul University, Istanbul, Turkey**

F. Aydogmus Sen, S. Cerci[66], B. Kaynak, S. Ozkorucuklu, D. Sunar Cerci[66]

**Institute for Scintillation Materials of National Academy of Science of Ukraine, Kharkov, Ukraine**

B. Grynyov

**National Scientific Center, Kharkov Institute of Physics and Technology, Kharkov, Ukraine**

L. Levchuk

**University of Bristol, Bristol, United Kingdom**

E. Bhal, S. Bologna, J.J. Brooke, E. Clement, D. Cussans, H. Flacher, J. Goldstein, G.P. Heath, H.F. Heath, L. Kreczko, B. Krikler, S. Paramesvaran, T. Sakuma, S. Seif El Nasr-Storey, V.J. Smith, J. Taylor, A. Titterton

**Rutherford Appleton Laboratory, Didcot, United Kingdom**

K.W. Bell, A. Belyaev[76], C. Brew, R.M. Brown, D.J.A. Cockerill, K.V. Ellis, K. Harder, S. Harper, J. Linacre, K. Manolopoulos, D.M. Newbold, E. Olaiya, D. Petyt, T. Reis, T. Schuh, C.H. Shepherd-Themistocleous, A. Thea, I.R. Tomalin, T. Williams

**Imperial College, London, United Kingdom**

R. Bainbridge, P. Bloch, S. Bonomally, J. Borg, S. Breeze, O. Buchmuller, A. Bundock, V. Cepaitis, G.S. Chahal[77], D. Colling, P. Dauncey, G. Davies, M. Della Negra, P. Everaerts, G. Fedi, G. Hall, G. Iles, J. Langford, L. Lyons, A.-M. Magnan, S. Malik, A. Martelli, V. Milosevic, J. Nash[78], V. Palladino, M. Pesaresi, D.M. Raymond, A. Richards, A. Rose, E. Scott, C. Seez, A. Shtipliyski, M. Stoye, A. Tapper, K. Uchida, T. Virdee[18], N. Wardle, S.N. Webb, D. Winterbottom, A.G. Zecchinelli, S.C. Zenz

**Brunel University, Uxbridge, United Kingdom**

J.E. Cole, P.R. Hobson, A. Khan, P. Kyberd, C.K. Mackay, I.D. Reid, L. Teodorescu, S. Zahid

**Baylor University, Waco, U.S.A.**

A. Brinkerhoff, K. Call, B. Caraway, J. Dittmann, K. Hatakeyama, A.R. Kanuganti, C. Madrid, B. McMaster, N. Pastika, S. Sawant, C. Smith

**Catholic University of America, Washington, DC, U.S.A.**

R. Bartek, A. Dominguez, R. Uniyal, A.M. Vargas Hernandez

**The University of Alabama, Tuscaloosa, U.S.A.**

A. Buccilli, O. Charaf, S.I. Cooper, S.V. Gleyzer, C. Henderson, P. Rumerio, C. West

**Boston University, Boston, U.S.A.**

A. Akpinar, A. Albert, D. Arcaro, C. Cosby, Z. Demiragli, D. Gastler, C. Richardson, J. Rohlf, K. Salyer, D. Sperka, D. Spitzbart, I. Suarez, S. Yuan, D. Zou

**Brown University, Providence, U.S.A.**

G. Benelli, B. Burkle, X. Coubez[19], D. Cutts, Y.t. Duh, M. Hadley, U. Heintz, J.M. Hogan[79], K.H.M. Kwok, E. Laird, G. Landsberg, K.T. Lau, J. Lee, M. Narain, S. Sagir[80], R. Syarif, E. Usai, W.Y. Wong, D. Yu, W. Zhang

**University of California, Davis, Davis, U.S.A.**

R. Band, C. Brainerd, R. Breedon, M. Calderon De La Barca Sanchez, M. Chertok, J. Conway, R. Conway, P.T. Cox, R. Erbacher, C. Flores, G. Funk, F. Jensen, W. Ko[†], O. Kukral, R. Lander, M. Mulhearn, D. Pellett, J. Pilot, M. Shi, D. Taylor, K. Tos, M. Tripathi, Y. Yao, F. Zhang

**University of California, Los Angeles, U.S.A.**

M. Bachtis, R. Cousins, A. Dasgupta, A. Florent, D. Hamilton, J. Hauser, M. Ignatenko, T. Lam, N. Mccoll, W.A. Nash, S. Regnard, D. Saltzberg, C. Schnaible, B. Stone, V. Valuev

**University of California, Riverside, Riverside, U.S.A.**

K. Burt, Y. Chen, R. Clare, J.W. Gary, S.M.A. Ghiasi Shirazi, G. Hanson, G. Karapostoli, O.R. Long, N. Manganelli, M. Olmedo Negrete, M.I. Paneva, W. Si, S. Wimpenny, Y. Zhang

**University of California, San Diego, La Jolla, U.S.A.**

J.G. Branson, P. Chang, S. Cittolin, S. Cooperstein, N. Deelen, M. Derdzinski, J. Duarte, R. Gerosa, D. Gilbert, B. Hashemi, D. Klein, V. Krutelyov, J. Letts, M. Masciovecchio, S. May, S. Padhi, M. Pieri, V. Sharma, M. Tadel, F. Würthwein, A. Yagil

**University of California, Santa Barbara — Department of Physics, Santa Barbara, U.S.A.**

N. Amin, C. Campagnari, M. Citron, A. Dorsett, V. Dutta, J. Incandela, B. Marsh, H. Mei, A. Ovcharova, H. Qu, M. Quinnan, J. Richman, U. Sarica, D. Stuart, S. Wang

**California Institute of Technology, Pasadena, U.S.A.**

D. Anderson, A. Bornheim, O. Cerri, I. Dutta, J.M. Lawhorn, N. Lu, J. Mao, H.B. Newman, T.Q. Nguyen, J. Pata, M. Spiropulu, J.R. Vlimant, S. Xie, Z. Zhang, R.Y. Zhu

**Carnegie Mellon University, Pittsburgh, U.S.A.**

J. Alison, M.B. Andrews, T. Ferguson, T. Mudholkar, M. Paulini, M. Sun, I. Vorobiev

**University of Colorado Boulder, Boulder, U.S.A.**

J.P. Cumalat, W.T. Ford, E. MacDonald, T. Mulholland, R. Patel, A. Perloff, K. Stenson, K.A. Ulmer, S.R. Wagner

**Cornell University, Ithaca, U.S.A.**

J. Alexander, Y. Cheng, J. Chu, D.J. Cranshaw, A. Datta, A. Frankenthal, K. Mcdermott, J. Monroy, J.R. Patterson, D. Quach, A. Ryd, W. Sun, S.M. Tan, Z. Tao, J. Thom, P. Wittich, M. Zientek

**Fermi National Accelerator Laboratory, Batavia, U.S.A.**

S. Abdullin, M. Albrow, M. Alyari, G. Apollinari, A. Apresyan, A. Apyan, S. Banerjee, L.A.T. Bauerdick, A. Beretvas, D. Berry, J. Berryhill, P.C. Bhat, K. Burkett, J.N. Butler, A. Canepa, G.B. Cerati, H.W.K. Cheung, F. Chlebana, M. Cremonesi, V.D. Elvira, J. Freeman, Z. Gecse, E. Gottschalk, L. Gray, D. Green, S. Grünendahl, O. Gutsche, R.M. Harris, S. Hasegawa, R. Heller, T.C. Herwig, J. Hirschauer, B. Jayatilaka, S. Jindariani, M. Johnson, U. Joshi, P. Klabbers, T. Klijnsma, B. Klima, M.J. Kortelainen, S. Lammel, D. Lincoln, R. Lipton, M. Liu, T. Liu, J. Lykken, K. Maeshima, D. Mason, P. McBride, P. Merkel, S. Mrenna, S. Nahn, V. O'Dell, V. Papadimitriou, K. Pedro, C. Pena[49], O. Prokofyev, F. Ravera, A. Reinsvold Hall, L. Ristori, B. Schneider, E. Sexton-Kennedy, N. Smith, A. Soha, W.J. Spalding, L. Spiegel, S. Stoynev, J. Strait, L. Taylor, S. Tkaczyk, N.V. Tran, L. Uplegger, E.W. Vaandering, H.A. Weber, A. Woodard

**University of Florida, Gainesville, U.S.A.**

D. Acosta, P. Avery, D. Bourilkov, L. Cadamuro, V. Cherepanov, F. Errico, R.D. Field, D. Guerrero, B.M. Joshi, M. Kim, J. Konigsberg, A. Korytov, K.H. Lo, K. Matchev, N. Menendez, G. Mitselmakher, D. Rosenzweig, K. Shi, J. Wang, S. Wang, X. Zuo

**Florida State University, Tallahassee, U.S.A.**

T. Adams, A. Askew, D. Diaz, R. Habibullah, S. Hagopian, V. Hagopian, K.F. Johnson, R. Khurana, T. Kolberg, G. Martinez, H. Prosper, C. Schiber, R. Yohay, J. Zhang

**Florida Institute of Technology, Melbourne, U.S.A.**

M.M. Baarmand, S. Butalla, T. Elkafrawy[14], M. Hohlmann, D. Noonan, M. Rahmani, M. Saunders, F. Yumiceva

**University of Illinois at Chicago (UIC), Chicago, U.S.A.**

M.R. Adams, L. Apanasevich, H. Becerril Gonzalez, R. Cavanaugh, X. Chen, S. Dittmer, O. Evdokimov, C.E. Gerber, D.A. Hangal, D.J. Hofman, C. Mills, G. Oh, T. Roy, M.B. Tonjes, N. Varelas, J. Viinikainen, X. Wang, Z. Wu

**The University of Iowa, Iowa City, U.S.A.**

M. Alhusseini, K. Dilsiz[81], S. Durgut, R.P. Gandrajula, M. Haytmyradov, V. Khristenko, O.K. Köseyan, J.-P. Merlo, A. Mestvirishvili[82], A. Moeller, J. Nachtman, H. Ogul[83], Y. Onel, F. Ozok[84], A. Penzo, C. Snyder, E. Tiras, J. Wetzel, K. Yi[85]

**Johns Hopkins University, Baltimore, U.S.A.**

O. Amram, B. Blumenfeld, L. Corcodilos, M. Eminizer, A.V. Gritsan, S. Kyriacou, P. Maksimovic, C. Mantilla, J. Roskes, M. Swartz, T.Á. Vámi

**The University of Kansas, Lawrence, U.S.A.**

C. Baldenegro Barrera, P. Baringer, A. Bean, A. Bylinkin, T. Isidori, S. Khalil, J. King, G. Krintiras, A. Kropivnitskaya, C. Lindsey, N. Minafra, M. Murray, C. Rogan, C. Royon, S. Sanders, E. Schmitz, J.D. Tapia Takaki, Q. Wang, J. Williams, G. Wilson

**Kansas State University, Manhattan, U.S.A.**

S. Duric, A. Ivanov, K. Kaadze, D. Kim, Y. Maravin, T. Mitchell, A. Modak, A. Mohammadi

**Lawrence Livermore National Laboratory, Livermore, U.S.A.**

F. Rebassoo, D. Wright

**University of Maryland, College Park, U.S.A.**

E. Adams, A. Baden, O. Baron, A. Belloni, S.C. Eno, Y. Feng, N.J. Hadley, S. Jabeen, G.Y. Jeng, R.G. Kellogg, T. Koeth, A.C. Mignerey, S. Nabili, M. Seidel, A. Skuja, S.C. Tonwar, L. Wang, K. Wong

**Massachusetts Institute of Technology, Cambridge, U.S.A.**

D. Abercrombie, B. Allen, R. Bi, S. Brandt, W. Busza, I.A. Cali, Y. Chen, M. D'Alfonso, G. Gomez Ceballos, M. Goncharov, P. Harris, D. Hsu, M. Hu, M. Klute, D. Kovalskyi, J. Krupa, Y.-J. Lee, P.D. Luckey, B. Maier, A.C. Marini, C. Mcginn, C. Mironov,

S. Narayanan, X. Niu, C. Paus, D. Rankin, C. Roland, G. Roland, Z. Shi, G.S.F. Stephans, K. Sumorok, K. Tatar, D. Velicanu, J. Wang, T.W. Wang, Z. Wang, B. Wyslouch

**University of Minnesota, Minneapolis, U.S.A.**

R.M. Chatterjee, A. Evans, S. Guts[†], P. Hansen, J. Hiltbrand, Sh. Jain, M. Krohn, Y. Kubota, Z. Lesko, J. Mans, M. Revering, R. Rusack, R. Saradhy, N. Schroeder, N. Strobbe, M.A. Wadud

**University of Mississippi, Oxford, U.S.A.**

J.G. Acosta, S. Oliveros

**University of Nebraska-Lincoln, Lincoln, U.S.A.**

K. Bloom, S. Chauhan, D.R. Claes, C. Fangmeier, L. Finco, F. Golf, J.R. González Fernández, I. Kravchenko, J.E. Siado, G.R. Snow[†], B. Stieger, W. Tabb, F. Yan

**State University of New York at Buffalo, Buffalo, U.S.A.**

G. Agarwal, C. Harrington, L. Hay, I. Iashvili, A. Kharchilava, C. McLean, D. Nguyen, A. Parker, J. Pekkanen, S. Rappoccio, B. Roozbahani

**Northeastern University, Boston, U.S.A.**

G. Alverson, E. Barberis, C. Freer, Y. Haddad, A. Hortiangtham, G. Madigan, B. Marzocchi, D.M. Morse, V. Nguyen, T. Orimoto, L. Skinnari, A. Tishelman-Charny, T. Wamorkar, B. Wang, A. Wisecarver, D. Wood

**Northwestern University, Evanston, U.S.A.**

S. Bhattacharya, J. Bueghly, Z. Chen, A. Gilbert, T. Gunter, K.A. Hahn, N. Odell, M.H. Schmitt, K. Sung, M. Velasco

**University of Notre Dame, Notre Dame, U.S.A.**

R. Bucci, N. Dev, R. Goldouzian, M. Hildreth, K. Hurtado Anampa, C. Jessop, D.J. Karmgard, K. Lannon, W. Li, N. Loukas, N. Marinelli, I. Mcalister, F. Meng, K. Mohrman, Y. Musienko[43], R. Ruchti, P. Siddireddy, S. Taroni, M. Wayne, A. Wightman, M. Wolf, L. Zygala

**The Ohio State University, Columbus, U.S.A.**

J. Alimena, B. Bylsma, B. Cardwell, L.S. Durkin, B. Francis, C. Hill, A. Lefeld, B.L. Winer, B.R. Yates

**Princeton University, Princeton, U.S.A.**

G. Dezoort, P. Elmer, B. Greenberg, N. Haubrich, S. Higginbotham, A. Kalogeropoulos, G. Kopp, S. Kwan, D. Lange, M.T. Lucchini, J. Luo, D. Marlow, K. Mei, I. Ojalvo, J. Olsen, C. Palmer, P. Piroué, D. Stickland, C. Tully

**University of Puerto Rico, Mayaguez, U.S.A.**

S. Malik, S. Norberg

**Purdue University, West Lafayette, U.S.A.**

V.E. Barnes, R. Chawla, S. Das, L. Gutay, M. Jones, A.W. Jung, B. Mahakud, G. Negro, N. Neumeister, C.C. Peng, S. Piperov, H. Qiu, J.F. Schulte, N. Trevisani, F. Wang, R. Xiao, W. Xie

**Purdue University Northwest, Hammond, U.S.A.**

T. Cheng, J. Dolen, N. Parashar, M. Stojanovic

**Rice University, Houston, U.S.A.**

A. Baty, S. Dildick, K.M. Ecklund, S. Freed, F.J.M. Geurts, M. Kilpatrick, A. Kumar, W. Li, B.P. Padley, R. Redjimi, J. Roberts[†], J. Rorie, W. Shi, A.G. Stahl Leiton, A. Zhang

**University of Rochester, Rochester, U.S.A.**

A. Bodek, P. de Barbaro, R. Demina, J.L. Dulemba, C. Fallon, T. Ferbel, M. Galanti, A. Garcia-Bellido, O. Hindrichs, A. Khukhunaishvili, E. Ranken, R. Taus

**Rutgers, The State University of New Jersey, Piscataway, U.S.A.**

B. Chiarito, J.P. Chou, A. Gandrakota, Y. Gershtein, E. Halkiadakis, A. Hart, M. Heindl, E. Hughes, S. Kaplan, O. Karacheban[22], I. Laflotte, A. Lath, R. Montalvo, K. Nash, M. Osherson, S. Salur, S. Schnetzer, S. Somalwar, R. Stone, S.A. Thayil, S. Thomas, H. Wang

**University of Tennessee, Knoxville, U.S.A.**

H. Acharya, A.G. Delannoy, S. Spanier

**Texas A&M University, College Station, U.S.A.**

O. Bouhali[86], M. Dalchenko, A. Delgado, R. Eusebi, J. Gilmore, T. Huang, T. Kamon[87], H. Kim, S. Luo, S. Malhotra, R. Mueller, D. Overton, L. Perniè, D. Rathjens, A. Safonov, J. Sturdy

**Texas Tech University, Lubbock, U.S.A.**

N. Akchurin, J. Damgov, V. Hegde, S. Kunori, K. Lamichhane, S.W. Lee, T. Mengke, S. Muthumuni, T. Peltola, S. Undleeb, I. Volobouev, Z. Wang, A. Whitbeck

**Vanderbilt University, Nashville, U.S.A.**

E. Appelt, S. Greene, A. Gurrola, R. Janjam, W. Johns, C. Maguire, A. Melo, H. Ni, K. Padeken, F. Romeo, P. Sheldon, S. Tuo, J. Velkovska, M. Verweij

**University of Virginia, Charlottesville, U.S.A.**

L. Ang, M.W. Arenton, B. Cox, G. Cummings, J. Hakala, R. Hirosky, M. Joyce, A. Ledovskoy, C. Neu, B. Tannenwald, Y. Wang, E. Wolfe, F. Xia

**Wayne State University, Detroit, U.S.A.**

P.E. Karchin, N. Poudyal, P. Thapa

**University of Wisconsin — Madison, Madison, WI, U.S.A.**

K. Black, T. Bose, J. Buchanan, C. Caillol, S. Dasu, I. De Bruyn, C. Galloni, H. He, M. Herndon, A. Hervé, U. Hussain, A. Lanaro, A. Loeliger, R. Loveless, J. Madhusu-

danan Sreekala, A. Mallampalli, D. Pinna, T. Ruggles, A. Savin, V. Shang, V. Sharma, W.H. Smith, D. Teague, S. Trembath-Reichert, W. Vetens

†: Deceased

1: Also at TU Wien, Wien, Austria

2: Also at Institute of Basic and Applied Sciences, Faculty of Engineering, Arab Academy for Science, Technology and Maritime Transport, Alexandria, Egypt, Alexandria, Egypt

3: Also at Université Libre de Bruxelles, Bruxelles, Belgium

4: Also at IRFU, CEA, Université Paris-Saclay, Gif-sur-Yvette, France

5: Also at Universidade Estadual de Campinas, Campinas, Brazil

6: Also at Federal University of Rio Grande do Sul, Porto Alegre, Brazil

7: Also at UFMS, Nova Andradina, Brazil

8: Also at Universidade Federal de Pelotas, Pelotas, Brazil

9: Also at University of Chinese Academy of Sciences, Beijing, China

10: Also at Institute for Theoretical and Experimental Physics named by A.I. Alikhanov of NRC 'Kurchatov Institute', Moscow, Russia

11: Also at Joint Institute for Nuclear Research, Dubna, Russia

12: Also at Helwan University, Cairo, Egypt

13: Now at Zewail City of Science and Technology, Zewail, Egypt

14: Also at Ain Shams University, Cairo, Egypt

15: Also at Purdue University, West Lafayette, U.S.A.

16: Also at Université de Haute Alsace, Mulhouse, France

17: Also at Erzincan Binali Yildirim University, Erzincan, Turkey

18: Also at CERN, European Organization for Nuclear Research, Geneva, Switzerland

19: Also at RWTH Aachen University, III. Physikalisches Institut A, Aachen, Germany

20: Also at University of Hamburg, Hamburg, Germany

21: Also at Department of Physics, Isfahan University of Technology, Isfahan, Iran

22: Also at Brandenburg University of Technology, Cottbus, Germany

23: Also at Skobeltsyn Institute of Nuclear Physics, Lomonosov Moscow State University, Moscow, Russia

24: Also at Institute of Physics, University of Debrecen, Debrecen, Hungary

25: Also at Physics Department, Faculty of Science, Assiut University, Assiut, Egypt

26: Also at MTA-ELTE Lendület CMS Particle and Nuclear Physics Group, Eötvös Loránd University, Budapest, Hungary

27: Also at Institute of Nuclear Research ATOMKI, Debrecen, Hungary

28: Also at IIT Bhubaneswar, Bhubaneswar, India

29: Also at Institute of Physics, Bhubaneswar, India

30: Also at G.H.G. Khalsa College, Punjab, India

31: Also at Shoolini University, Solan, India

32: Also at University of Hyderabad, Hyderabad, India

33: Also at University of Visva-Bharati, Santiniketan, India

34: Also at Indian Institute of Technology (IIT), Mumbai, India

35: Also at Deutsches Elektronen-Synchrotron, Hamburg, Germany

36: Also at Department of Physics, University of Science and Technology of Mazandaran, Behshahr, Iran

37: Now at INFN Sezione di Bari [a], Università di Bari [b], Politecnico di Bari [c], Bari, Italy

38: Also at Italian National Agency for New Technologies, Energy and Sustainable Economic Development, Bologna, Italy

82: Also at Georgian Technical University, Tbilisi, Georgia

83: Also at Sinop University, Sinop, Turkey

84: Also at Mimar Sinan University, Istanbul, Istanbul, Turkey

85: Also at Nanjing Normal University Department of Physics, Nanjing, China

86: Also at Texas A&M University at Qatar, Doha, Qatar

87: Also at Kyungpook National University, Daegu, Korea